AD-A093 259 AERONAUTICAL RESEARCH LABS MELBOURNE (AUSTRALIA) F/G 1/3
PROPELLER WHIRL FLUTTER CALCULATIONS FOR THE N22 NOMAD PRODUCTI--ETC(U)
MAY 79 B EMSLIE, P M COX
UNCLASSIFIED ARL/STRUC NOTE-452 NL

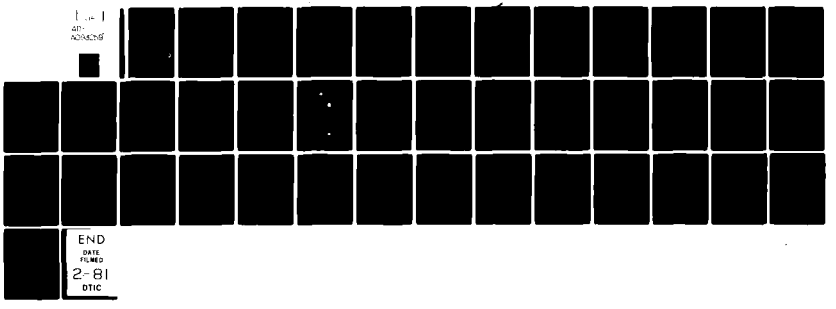

END
DATE FILMED
2-81
DTIC

ARL-STRUC-NOTE-452

AR-001-738

DEPARTMENT OF DEFENCE

DEFENCE SCIENCE AND TECHNOLOGY ORGANISATION

AERONAUTICAL RESEARCH LABORATORIES

MELBOURNE, VICTORIA

STRUCTURES NOTE 452

PROPELLER WHIRL FLUTTER CALCULATIONS FOR THE N22 NOMAD PRODUCTION AIRCRAFT

by

BETTY EMSLIE and PETRA M. COX

COPY No 11

MAY 1979

AR-001-738

DEPARTMENT OF DEFENCE
DEFENCE SCIENCE AND TECHNOLOGY ORGANISATION
AERONAUTICAL RESEARCH LABORATORIES

STRUCTURES NOTE-452

PROPELLER WHIRL FLUTTER CALCULATIONS FOR THE N22 NOMAD PRODUCTION AIRCRAFT

by

BETTY EMSLIE and PETRA M. COX

SUMMARY

Propeller whirl flutter speeds have been calculated for the N22 Nomad production aircraft. These calculated flutter speeds lie well outside the aircraft's flight envelope.

POSTAL ADDRESS: Chief Superintendent, Aeronautical Research Laboratories,
Box 4331, P.O., Melbourne, Victoria, 3001, Australia.

DOCUMENT CONTROL DATA SHEET

Security classification of this page: Unclassified

1. Document Numbers
   (a) AR Number: AR-001-738
   (b) Document Series and Number: Structures Note 452
   (c) Report Number: ARL-Struc-Note--452

2. Security Classification
   (a) Complete document: Unclassified
   (b) Title in isolation: Unclassified
   (c) Summary in isolation: Unclassified

3. Title: PROPELLER WHIRL FLUTTER CALCULATIONS FOR THE N22 NOMAD PRODUCTION AIRCRAFT

4. Personal Author(s):
   Emslie, Betty
   Cox, Petra M.

5. Document Date: May, 1979

6. Type of Report and Period Covered:

7. Corporate Author(s):
   Aeronautical Research Laboratories

8. Reference Numbers
   (a) Task: AUS 73/2
   (b) Sponsoring Agency: DSTP 10

9. Cost Code: 23-5000

10. Imprint:
    Aeronautical Research Laboratories, Melbourne

11. Computer Program(s)
    (Title(s) and language(s)):

12. Release Limitations (of the document)
    Approved for public release

12-0. Overseas:	N.O.		P.R.	1	A		B		C		D		E	

13. Announcement Limitations (of the information on this page):
    No Limitations

14. Descriptors:

Flutter	Pitching	
Aircraft propellers	Mathematical models	
Vibration tests	Nomad aircraft	
Yaw		

15. Cosati Codes:

0103	
1402	
1201	

16. *ABSTRACT*

Propeller whirl flutter speeds have been calculated for the N22 Nomad production aircraft. These calculated flutter speeds lie well outside the aircraft's flight envelope.

CONTENTS

NOTATION

I_Q	Polar moment of inertia of the propeller and the rotating engine parts, slug ft^2 (kg m^2).
I_{PD}	Moment of inertia of the propeller about a diameter, slug ft^2 (kg m^2).
K_i	Generalised stiffness terms.
M	Mach number of the free stream.
M_{iP}	Propeller generalised mass terms.
M_{iW}	Wing generalised mass terms.
$Q'_{ij} + ivQ''_{ij}$	Generalised aerodynamic force coefficient.
V_D	Design dive speed, ft/sec (m/sec).
X, Y, Z	Rectangular cartesian co-ordinate axis system (see Figs 2*a* and 2*b*).
γ_i	Fraction of critical damping present in mode i.
θ	Pitch angular displacement at the propeller hub at time t, rad.
θ_1	Angular displacement in pitch per unit linear displacement at the propeller hub, rad/ft (rad/m).
ν	Frequency parameter.
ψ	Yaw angular displacement at the propeller hub at time t, rad.
ψ_1	Angular displacement in yaw per unit linear displacement at the propeller hub, rad/ft (rad/m).
Ω	Propeller rotational speed, rad/sec.

1. INTRODUCTION

Propeller whirl calculations for the Government Aircraft Factories' N22 Nomad production aircraft (see Fig. 1) were carried out at the request of G.A.F. in order to meet the requirements of Federal Aviation Regulations 23.629. The production version is considerably different from the prototype; the main differences being summarised below.

1. The wing, ailerons, flaps and spoilers are lighter.
2. The fin and rudder are lighter though larger.
3. The fuselage is lighter.
4. The stub-wing and undercarriage are lighter and twin wheels are fitted.
5. The tailplane and rudder tabs are bigger.
6. The engine nacelles are lighter.

2. OUTLINE OF ANALYSIS

As in Reference 2, the wing, engine, nacelle and propeller are idealised as a two degree of freedom system, where pitch and yaw of the engine and nacelle structure are the two degrees of freedom allowed. The analytical model considered is illustrated in Figures 2(*a*), 2(*b*) and 2(*c*). Wing flexibility is included in the equations and both propeller and wing aerodynamic forces are taken into account. However, nacelle aerodynamic forces and aerodynamic interference effects between the wing and the propeller are neglected.

The equations of motion for this model are derived and their solution is discussed in Appendix A, Reference 2. The notation of Reference 2 will be used throughout this report.

As in Reference 2, all computations were carried out on the Aeronatuical Research Laboratories' PDP10 computer and the same major programs VA01BE and VA02BE were used.

3. DISCUSSION OF THE DATA USED IN THE ANALYSIS

3.1 Data Obtained from the Ground Vibration Test

A ground vibration test was carried out on the production version N22 Nomad aircraft by Aeronautical Research Laboratories' staff (Ref. 3).

At first, four modes involving significant engine pitch and two modes involving engine yaw were identified. As in the resonance test on the prototype Nomad, the lower frequency engine yaw mode was not well defined. Hence, two versions of this mode were considered in the calculations. These six modes have natural frequencies at 6·51, 8·85, 10·64 and 15·40 Hz (pitch) 6·48 (*a*), 6·48 (*b*) and 13·795 Hz (yaw). (see Figs 6–13 and Figs 16–17).

A subsequent review of the ground vibration test results suggested that the 6·01 and 18·14 Hz modes also involved significant engine pitch motion (see Figs 4, 5, 14, 15). Therefore, whirl flutter calculations including these modes were also carried out.

The positions of the engine nodes in each of the above modes are tabulated in Table 4.

In each of the modes involving engine pitch, there is some wing motion. On the other hand, there is no wing motion in any of the engine yaw modes.

Estimates of γ_i, the fraction of critical damping present in mode "i", were obtained during the resonance test. These values are included in Table 4.

3.2 Inertia and Geometric Data

Initially, all the relevant inertia and geometric data required for the N22 Nomad propeller whirl flutter calculations were not available from the Government Aircraft Factories. The problem area was the N22 engine nacelle structure and cowling. Although the N22 nacelle

structure and the engine nacelle cowling were known to be lighter than those of the Nomad prototype, no list of components with their mass and c.g. location was immediately available for the N22 aircraft. Since the propeller whirl flutter calculations could not proceed without this data, a discussion was held with staff from the Government Aircraft Factories. During this discussion it was requested that the inertia distribution for the Nomad prototype nacelle structure and engine nacelle cowling be used (see Tables 1(*b*) and 1(*c*)).

This was thought to be a reasonable assumption since it was expected that the nacelle structure and the engine nacelle cowling would contribute less than 10% to the generalised mass of the nonrotating engine-nacelle-propeller system. When the generalised mass calculations were completed it was found that the nacelle structure and the engine nacelle cowling contribution to $M_{2P} \cdot I_{PD}\theta_1^2$ was 34·6% for the 18·14 Hz mode, 6·7% for the 10·64 Hz mode and 6·1% for the 15·40 Hz mode. For all the other modes considered the nacelle structure and the engine nacelle cowling contribution represented less than 4% of the generalised mass of the engine-nacelle-propeller system.

It was also requested by the Government Aircraft Factories that some propeller whirl calculations be carried out with the mass of each item of the nacelle structure and the engine nacelle cowling equal to 75% of the value listed in Tables 1(*b*) and 1(*c*). This was done and the results are discussed in Section 4.4.

Subsequently, a further mass distribution was supplied by the Government Aircraft Factories. Here the nacelle structure and the engine nacelle cowling were idealised as 8 point masses (see Table 1(*d*)). Propeller whirl flutter calculations were carried out for this mass distribution and the results are discussed in Section 4.4.

The engine installation for the N22 was considered to be essentially the same as for the Nomad prototype (see Table 1(*a*)).

The N22 propeller is the same as the Nomad prototype propeller (see Fig. 3 and Table 2).

The N22 wing is idealised in the same way as the Nomad prototype wing. That is, the wing is assumed to consist of 20 rigid strips. Table 3 lists the wing mass and moment of inertia distribution. When comparing the N22 wing with the Nomad prototype wing (Table 3, Ref. 2), it should be noted that the strip between 10·8 ft and 12·0 ft cannot be compared directly. In the Nomad prototype calculations the strut and stub wing were included in this strip. Subsequently the computer programs for the generalised mass of the wing were improved and now the strut and stub wing contributions are added in separately.

4. FLUTTER CALCULATIONS

4.1 General

Propeller whirl flutter speeds for the N22 Nomad production aircraft were calculated using the matrix equation of motion (A25) of Reference 2.

Initially wing contributions were not included in the equations of motion. This corresponds to a simplified model in which the engine-nacelle-propeller system is mounted on a rigid wing. Using this simplified model, calculations were performed for each of the eighteen possible binary combinations of the three yaw modes and the six modes showing significant engine pitch motion (see Table 5). Two altitudes were considered, sea level and 22,000 feet. In each of these calculations structural damping was assumed to be zero.

The results of these flutter calculations are presented in Table 6. Examination of Tables 5 and 6 reveals that for each pitch mode coupled with either version of the 6·48 Hz yaw mode the flutter speed is many knots higher than the flutter speed for the same pitch mode coupled with the 13·79 Hz yaw mode. This was to be expected, because Reed in Reference 5 and many other investigators have demonstrated the significant stabilising influence of moving the pivot axes (i.e. the engine nodes) aft. Reference to Table 4 shows that both versions of the 6·48 Hz yaw mode have engine node locations more than 70 inches aft of the engine node location for the 13·79 Hz yaw mode. Therefore it would be sufficient to demonstrate that the binary combinations of the 13·79 Hz yaw mode with each of the six modes showing significant engine pitch motion have flutter speeds that lie outside the N22 Nomad aircraft's flight envelope.

Further, no more flutter calculations were carried out for binary B 15·0, the combination of the 13·79 Hz yaw mode with the 6.01 Hz mode. This arose because the 6.01 Hz mode is

anti-symmetric wing bending and the 6·51 Hz mode is symmetric wing bending (see Table 1, Ref. 3). In the present calculations, where a single powerplant on a wing is being considered (see Fig. 2) binaries B 3·0 and B 15·0 are very similar. See Table 5 and compare Figures 4 and 5 with Figures 6 and 7. However the location of the engine node in the 6·01 Hz mode is 6 inches aft of the location of the engine node in the 6·51 Hz mode. Again the stabilizing influence of an aft engine node is evident, for flutter speeds calculated for binary B 15·0 are greater than the corresponding flutter speeds calculated for binary B 3·0. For this reason it was sufficient to consider binary B 3·0 in further calculations.

4.2 Calculation of Flutter Speeds for the Realistic Model which Includes Wing Contributions in the Equations of Motion

As is pointed out in Reference 5, simplified models such as an engine-nacelle-propeller system mounted on a rigid wing are useful for demonstrating basic features of propeller whirl flutter. However, in order to evaluate the propeller whirl flutter characteristics of an actual aircraft a more realistic model, in which the engine-nacelle-propeller system is mounted on the flexible wing of the aircraft, must be used. This means that wing contributions must be included in the equations of motion (A25 of Ref. 2).

In the previous section it was shown that it would be sufficient for further flutter calculations to be concentrated on binary combinations B 3·0, B 6·0, B 9·0, B 12·0 and B 18·0. When wing contributions have been included in the equations of motion these binary combinations are renamed B 3·1, B 6·1, B 9·1, B 12·1 and B 18·1 (see Table 7). Wing generalised aerodynamic force coefficients Q'_{22} and Q''_{22} were calculated using unsteady lifting surface computer programs (see Ref. 4). These generalised aerodynamic force coefficients Q'_{22} and Q''_{22} are functions of Mach number M and frequency parameter ν. $M = 0{\cdot}3$ was chosen as appropriate for the N22 Nomad and a number of different values of ν were considered (see Table 8).

The flutter speeds calculated for this realistic model of the N22 Nomad production aircraft are presented in Table 9 and are well in excess of V_D, the design dive speed (235 knots E.A.S.).

Comparison of Tables 6 and 9 shows that the flutter speeds calculated for the realistic model, which includes wing contributions in the equations of motion, are very much higher than the corresponding flutter speeds calculated for the simplified model, where no wing contributions are included in the equations of motion. Other investigations have also shown that when an engine-nacelle-propeller system is mounted on a flexible wing the whirl flutter speed is generally higher than if the system were mounted on a rigid back-up structure (see Ref. 5).

4.3 Use of the Simplified Model to Show the Effect of Including Measured Structural Damping

Because the flutter speeds for the realistic model, even with zero structural damping, were so high (see Table 9) it is not possible to use this model to demonstrate the effect of including measured structural damping in the equations of motion. Therefore it was necessary to use the simplified model which has no wing terms included in the equations of motion.

Estimates of modal damping were obtained during the ground vibration test (see Table 4). For binaries B 3·0, B 6·0, B 9·0, B 12·0 and B 18·0 boundaries corresponding to one quarter and one half the measured values of damping are plotted in Figures 18–22. Where a boundary is not included, the flutter speeds have exceeded the 400 knots E.A.S. limit of these graphs.

Although the flutter boundaries plotted in Figures 18–22 were calculated using the simplified model, with no wing terms included in the equations of motion, they do give an indication of the extent to which the propeller whirl flutter speeds are increased when measured structural damping is included in the equations of motion.

4.4 Use of the Simplified Model to Show the Effect of Variations in the Mass of the Nacelle Structure and the Engine Nacelle Cowling

As in the previous section, because the flutter speeds for the realistic model were so high, the simplified model had to be used to demonstrate the effect of variations in the mass of the nacelle structure and the engine nacelle cowling.

As was pointed out in Section 3.2, all the calculations so far have been carried out using the mass distribution for the Nomad prototype nacelle structure and engine nacelle cowling.

For binaries B 6·0, B 9·0, B 12·0 and B 18·0, some flutter speeds were also calculated using the two lighter mass distributions for the nacelle structure and engine nacelle cowling. The mass distribution, in which the mass of each item of the nacelle structure and engine nacelle cowling is equal to 75% of the value listed in Tables 1(*b*) and 1(*c*) will be referred to as nacelle model A. The mass distribution, in which the nacelle structure and engine nacelle cowling are idealised as 8 point masses, will be referred to as nacelle model B.

The flutter speeds calculated for binaries B 6·0, B 9·0 and B 12·0 using either nacelle model A or B differ from those calculated using the Nomad prototype nacelle mass by less than 1%. For binary B 18·0 calculations using nacelle model A showed a 4% decrease in flutter speed and calculations using nacelle model B showed an increase of 6%. Although the total mass of nacelle model B is slightly less than the total mass of nacelle model A, the generalised mass and hence the generalised stiffness of nacelle model B is greater than that of nacelle model A. It is this increase in generalised stiffness that leads to the higher flutter speed for nacelle model B.

As was expected, in most cases the variations in the mass of the nacelle structure and engine nacelle cowling made little difference to the calculated flutter speeds. However, it is recommended that, in future, propeller whirl flutter speeds be calculated using nacelle model A.

5. CONCLUSIONS

Propeller whirl flutter speeds have been calculated for the N22 Nomad production aircraft. Reference to Table 9, where these propeller whirl flutter speeds are tabulated, shows that they lie well outside the aircraft's flight envelope.

Because the propeller whirl flutter speeds calculated for the N22 Nomad production aircraft were so high, a simplified model was used to demonstrate the effects on flutter speed of engine node location, structural damping and variations in the mass of the nacelle structure and the engine nacelle cowling. The results of these calculations for the simplified model show clearly the stabilising influence of an aft engine node location. When amounts of structural damping equal to one quarter and one half the measured values were included in the equations for the simplified model, the calculated flutter speeds were increased considerably even for these small amounts of structural damping. These effects on flutter speed of engine node location and structural damping are consistent with the findings of previous propeller whirl studies. As was expected the variations in the mass of the nacelle structure made little difference to the calculated flutter speeds.

ACKNOWLEDGEMENT

The cooperation of members of the staff of the Government Aircraft Factories, particularly Mr I. Herszberg and Mr P. Buchler, is gratefully acknowledged.

REFERENCES

1. — Federal Aviation Regulations, Vol. III, Part 23. Airworthiness Standards. Normal, Utility and Aerobatic Category Airplanes. Issued by Department of Transportation. Federal Aviation Administration, 1969.

2. Emslie, Betty Propeller Whirl Flutter Calculations for the Nomad Aircraft. Note ARL/SM 402, 1974.

3. Long, G. and Cox, Petra M. Resonance Test on Nomad Production Version. Tech. Memo. ARL/Struc. 230, 1975.

4. Long, G. An Improved Method for Calculating Generalised Airforces on Oscillating Wings in Subsonic Flow. A.R.C. R & M 3657, 1969.

5. Reed, W. H. Propeller-Rotor Whirl Flutter AGARD Manual on Aeroelasticity, Vol. III, Ch. 9, 1967.

TABLE 1 (A)
Engine Installation

Item	Mass (Slug)	X Axis Arm (In.)
Engine (Bare) (Port)	6·06	154·9
Engine Mounts (3 off)	0·13	152·2
Tacho Gen (2 off)	0·11	15[illegible]·3
Oil Tank	0·21	14[illegible]·0
Oil Tank Supports	0·05	146·2
Oil Cooler (Bolts and Flange)	0·30	171·7
Oil Pipes	0·21	152·2
Oil (Miscellaneous)	0·01	152·2
Oil Press. Transmitter (Torque)	0·02	144·2
Oil Press. Transmitter (Engine)	0·02	144·2
Oil Cooler Duct Fixed	0·06	180·0
Oil Temp. Bulb	0·01	168·0
Propeller	3·84	131·8
Starter Gen. (Port)	0·53	159·9
Fuel Line to Fire Wall	0·03	174·0
Fire Warning Transmitter	0·05	164·0
Fire Extinguish Nozzle	0·01	179·0
Drain Branch Assembly	0·01	165·0
Miscellaneous	0·18	152·2
Compressor Bleed Assembly	0·02	168·0
Flexible Connector	0·05	152·2
Total	11·91	147·9

TABLE 1 (B)
Nacelle Structure

Item	Mass (Slug)	X Axis Arm (In.)
Riveted Structure 1	0·31	168·0
Riveted Structure 2	0·75	180·9
Rear Fairing	0·05	206·0
Bottom Support	0·16	168·6
Yoke Assembly	0·34	152·0
Mounting Brackets (2 off)	0·22	182·2
Tie Rod Assembly	0·10	163·1
Miscellaneous	0·01	171·4

TABLE 1 (C)
Engine Nacelle Cowling

Item	Mass (Slug)	X Axis Arm (In.)
Upper Front Fairing	0·05	142·0
Lower Front Fairing	0·11	144·0
Coupling	0·02	139·0
Top Cowl	0·30	165·0
Lower Cowl	0·27	161·0
Miscellaneous	0·01	158·3

TABLE 1 (D)
Nacelle Structure and Engine Nacelle Cowling

Section	Mass (Slug)	X Axis Arm (In.)
1	0·20	141·0
2	0·37	152·0
3	0·10	156·3
4	0·09	162·8
5	0·11	168·2
6	0·11	173·6
7	0·25	178·7
8	0·61	194·2

TABLE 2
Propeller Data

I_Q	4·8415 Slug ft^2
I_{PD}	2·267 Slug ft^2
Ω	2025 RPM 212·06 Rad/Sec.

TABLE 3
Wing Mass and Moment of Inertia Distribution

Inboard Edge of Strip (ft)	Outboard Edge of Strip (ft)	Mass of Strip (Slug)	Moment of Inertia of Strip About Its C.G. (Slug ft²)	Distance of Strip C.G. Aft of Front Spar (ft)
0·0	1·2	2·68	2·84	1·34
1·2	2·4	2·68	3·49	1·53
2·4	3·6	2·43	2·59	1·40
3·6	4·8	2·45	2·38	1·36
4·8	6·0	2·38	2·35	1·37
6·0	7·2	2·40	2·40	1·44
7·2	8·4	2·27	2·16	1·40
8·4	9·6	2·26	2·34	1·45
9·6	10·8	0·95	1·73	2·09
10·8	12·0	0·87	1·89	1·36
12·0	13·2	0·69	1·63	1·18
13·2	14·4	0·63	1·74	1·84
14·4	15·6	0·50	0·94	1·83
15·6	16·8	0·38	0·78	1·59
16·8	18·0	0·43	0·82	1·76
18·0	19·2	0·34	0·66	1·86
19·2	20·4	0·43	0·76	1·99
20·4	21·6	0·35	0·73	1·78
21·6	22·8	0·54	0·86	2·32
22·8	24·0	0·33	0·66	1·89

TABLE 4
Modal Data

Description of Engine Motion	Position of Node Relative to Engine Support Yoke	Natural Frequency (Hz)	Damping (% Critical)
Engine Pitch	25·0 Inches Aft	6·01	1·4
Engine Pitch	19·0 Inches Aft	6·51	1·8
Engine Pitch	5·0 Inches Aft	8·85	2·1
Engine Pitch	5 5 Inches Ahead	10·64	2·4
Engine Pitch	16·0 Inches Ahead	15·40	1·4
Engine Pitch	7·0 Inches Ahead	18·14	2·2
Engine Yaw A	68·0 Inches Aft	6·48	2·2
Engine Yaw B	90·0 Inches Aft	6·48	2·2
Engine Yaw	7·0 Inches Ahead	13·79	3·7

TABLE 5
Binary Combinations of the Pitch and Yaw Modes
No Wing Contributions in the Equations of Motion

Binary	M_{1P}	M_{2P}	ψ_1	θ_1	K_1	$K=(K_2/K_1)$
B 1·0 Yaw 6·48 Hz Pitch 6·51 Hz	8·650	5·919	0·1360	0·3062	14400	0·7119
B 2·0 Yaw 6·48 Hz Pitch 6·51 Hz	9·546	5·919	0·1089	0·3062	15900	0·6465
B 3·0 Yaw 13·79 Hz Pitch 6·51 Hz	15·238	5·919	0·9091	0·3062	128500	0·0799
B 4·0 Yaw 6·48 Hz Pitch 8·85 Hz	8·650	5·493	0·1360	0·4762	14400	1·2890
B 5·0 Yaw 6·48 Hz Pitch 8·85 Hz	9·546	5·493	0·1089	0·4762	15900	1·1705
B 6·0 Yaw 13·79 Hz Pitch 8·85 Hz	15·238	5·493	0·9091	0·4762	128500	0·1446
B 7·0 Yaw 6·48 Hz Pitch 10·64 Hz	8·650	12·749	0·1360	0·8163	14400	4·4229
B 8·0 Yaw 6·48 Hz Pitch 10·64 Hz	9·546	12·749	0·1089	0·8163	15900	4·0163
B 9·0 Yaw 13·79 Hz Pitch 10·64 Hz	15·238	12·749	0·9091	0·8163	128500	0·4961
B10·0 Yaw 6·48 Hz Pitch 15·40 Hz	8·650	275·745	0·1360	2·8569	14400	191·1905
B11·0 Yaw 6·48 Hz Pitch 15·40 Hz	9·546	275·745	0·1089	2·8569	15900	173·6133
B12·0 Yaw 13·79 Hz Pitch 15·40 Hz	15·238	275·745	0·9091	2·8569	128500	21·4456
B13·0 Yaw 6·48 Hz Pitch 6·01 Hz	8·650	6·390	0·1360	0·2655	14400	0·6482
B14·0 Yaw 6·48 Hz Pitch 6·01 Hz	9·546	6·390	0·1089	0·2655	15900	0·5886
B15·0 Yaw 13·79 Hz Pitch 6·01 Hz	15·238	6·390	0·9091	0·2655	128500	0·0727
B16·0 Yaw 6·48 Hz Pitch 18·14 Hz	8·650	24·069	0·1360	0·9091	14400	23·3882
B17·0 Yaw 6·48 Hz Pitch 18·14 Hz	9·546	24·069	0·1089	0·9091	15900	21·2380
B18·0 Yaw 13·79 Hz Pitch 18·14 Hz	15·238	24·069	0·9091	0·9091	128500	2·6234

TABLE 6
Summary of Binary Results
No Wing Contributions in the Equations of Motion
Zero Structural Damping

Binary	Flutter Speed Knots E.A.S.			
	Propeller Blade Lift Curve Slope 2π		With Aerodynamic Corrections	
	Sea Level	22,000 ft	Sea Level	22,000 ft
B 1·0	>890	304	415	264
B 2·0	>890	630	415	295
B 3·0	294	209	291	206
B 4·0	358	288	344	255
B 5·0	498	457	415	295
B 6·0	214	151	216	154
B 7·0	686	630	415	295
B 8·0	890	630	415	295
B 9·0	194	137	197	140
B10·0	890	630	415	295
B11·0	890	630	415	295
B12·0	233	164	236	168
B13·0	890	630	415	295
B14·0	890	630	415	295
B15·0	383	275	366	256
B16·0	890	630	415	295
B17·0	890	630	415	295
B18·0	280	198	285	203

TABLE 7
Binary Combinations of the Pitch and Yaw Modes
Wing Contributions are Included in the Equations of Motion

Binary	$M_{1P} + M_{1W}$ ($M_{1W} = 0$)	$M_{2P} + M_{2W}$	ψ_1	θ_1	K_1	$K = (K_2/K_1)$
B 3·1 Yaw 13·79 Hz Pitch 6·51 Hz	15·238	7·701	0·9091	0·3062	128600	0·1030
B 6·1 Yaw 13·79 Hz Pitch 8·85 Hz	15·238	18·759	0·9091	0·4762	128600	0·4636
B 9·1 Yaw 13·79 Hz Pitch 10·64 Hz	15·238	28·658	0·9091	0·8163	128600	1·0488
B12·1 Yaw 13·79 Hz Pitch 15·40 Hz	15·238	968·008	0·9091	2·8569	128600	71·8476
B18·1 Yaw 13·79 Hz Pitch 18·14 Hz	15·238	646·106	0·9091	0·9091	128600	65·4794

TABLE 8
Wing Generalised Aerodynamic Force Coefficients
$M = 0·3$

Modal Frequency	ν	Q'_{22}	Q''_{22}
6·51 Hz	0·001	−0·203403	−0·496435
	0·1	−0·190580	−0·597241
	0·2	0·169647	−0·646083
	0·3	0·142194	−0·669829
8·85 Hz	0·001	−1·306722	−4·880833
	0·1	−1·240116	−5·220880
	0·2	1·097227	−5·373148
	0·3	0·880213	−5·445278
10·64 Hz	0·001	0·575231	−3·531347
	0·1	0·543176	−3·546074
	0·2	0·450659	−3·562088
	0·3	0·298256	−3·571111
15·40 Hz	0·001	6·469120	109·150463
	0·1	5·724306	108·817130
	0·2	3·389023	108·503241
	0·3	0·605255	108·387963
18·14 Hz	0·001	23·830277	171·137030
	0·1	24·821527	169·109720
	0·2	27·943425	169·291700
	0·3	33·134861	169·449070

TABLE 9
Summary of Binary Results
Wing Contributions are Included in the Equations of Motion
Zero Structural Damping

Assumed $M = 0{\cdot}3$

Binary	Assumed ν	Flutter Speed Knots E.A.S.			
		Propeller Blade Lift Curve Slope $= 2\pi$		With Aerodynamic Corrections	
		Sea Level	22,000 ft	Sea Level	22,000 ft
B 3·1	0·001	890	630	415	295
B 3·1	0·1	890	630	415	295
B 6·1	0·001	890	630	415	295
B 6·1	0·1	890	630	415	295
B 9·1	0·001	865	630	415	295
B 9·1	0·1	877	630	415	295
B12·1	0·001	890	630	415	295
B12·1	0·1	890	630	415	295
B18·1	0·001	890	630	415	295
B18·1	0·1	890	630	415	295

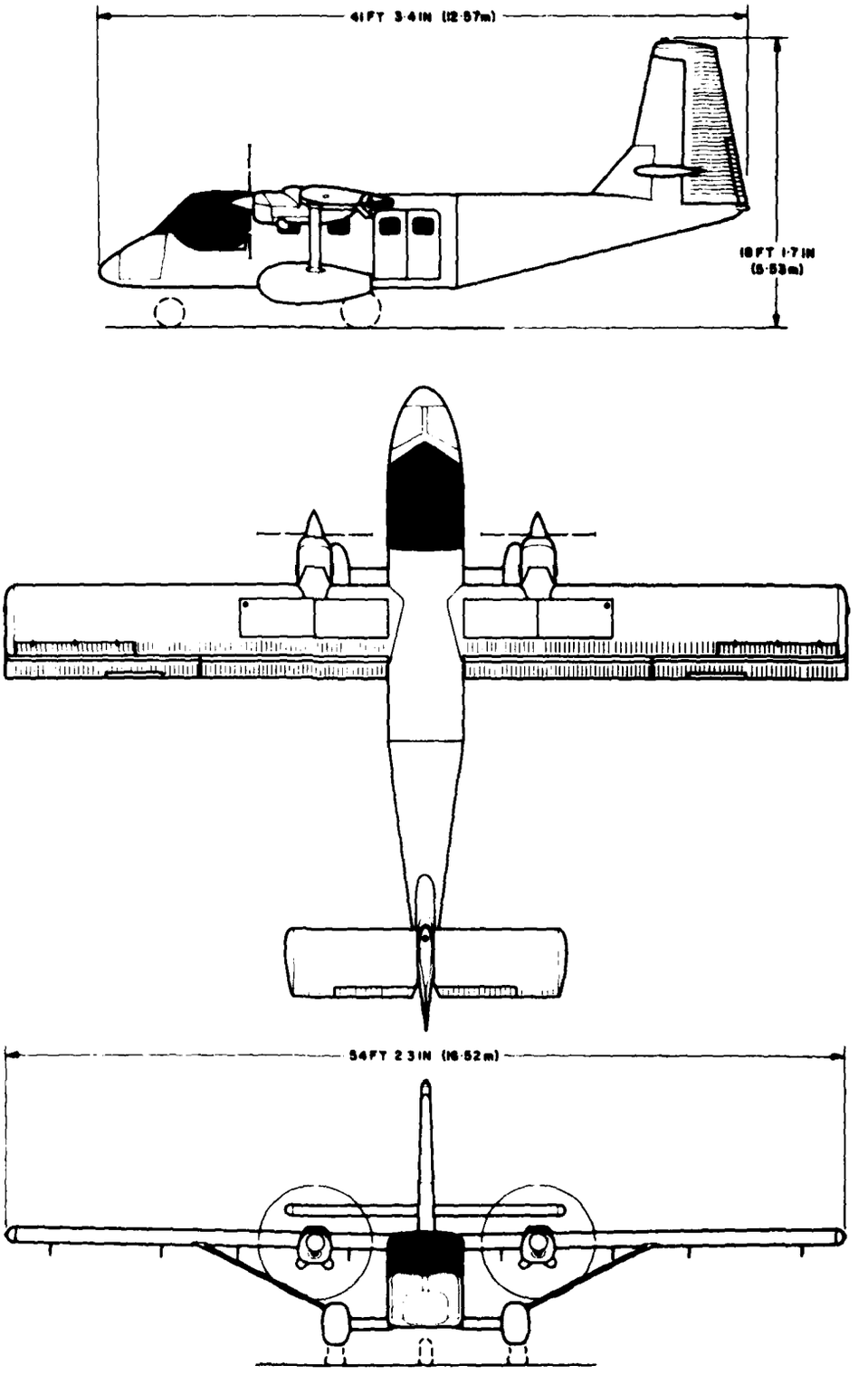

FIG. 1 : G.A.F. MODEL N22

Fig. 2 (a)

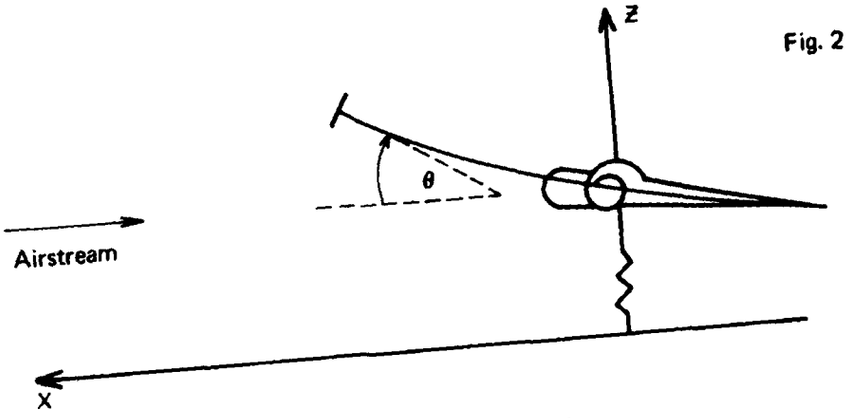

Section at propeller station

Fig. 2 (b)

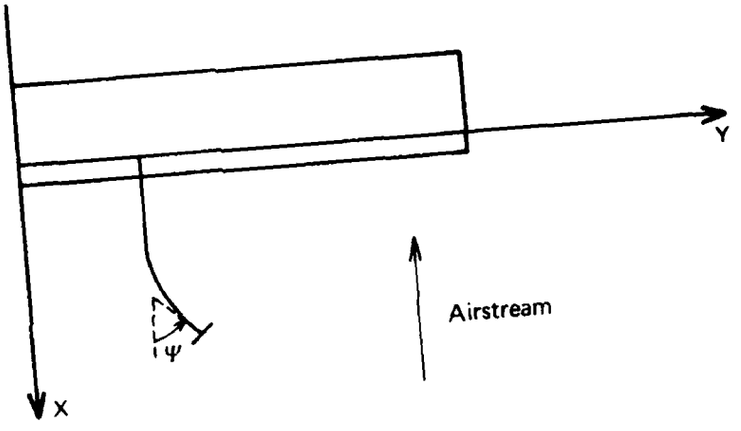

Plan view

Fig. 2 (c)

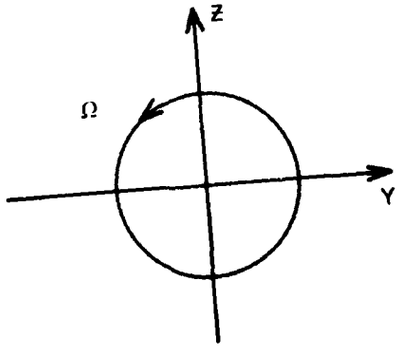

Direction of propeller rotation

FIGS. 2a, b, c COORDINATE SYSTEM USED IN THE ANALYSIS

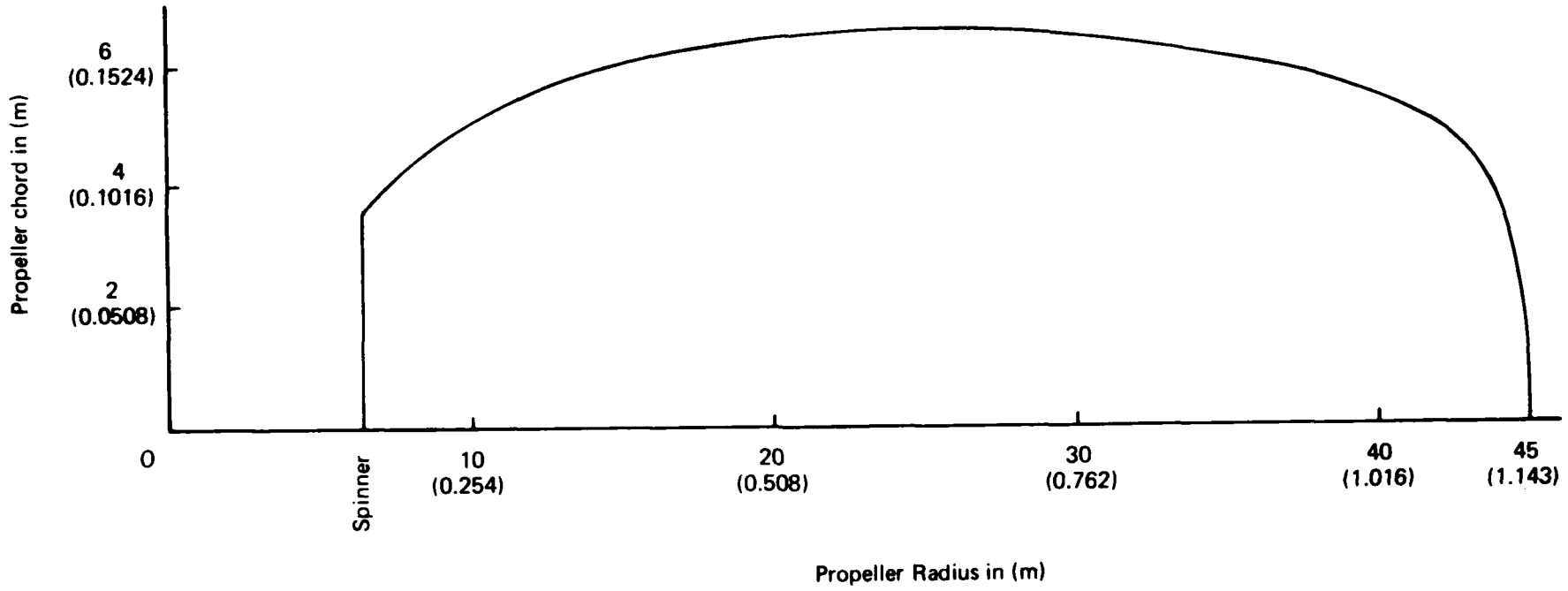

FIG. 3 PROPELLER CHORD VARIATION

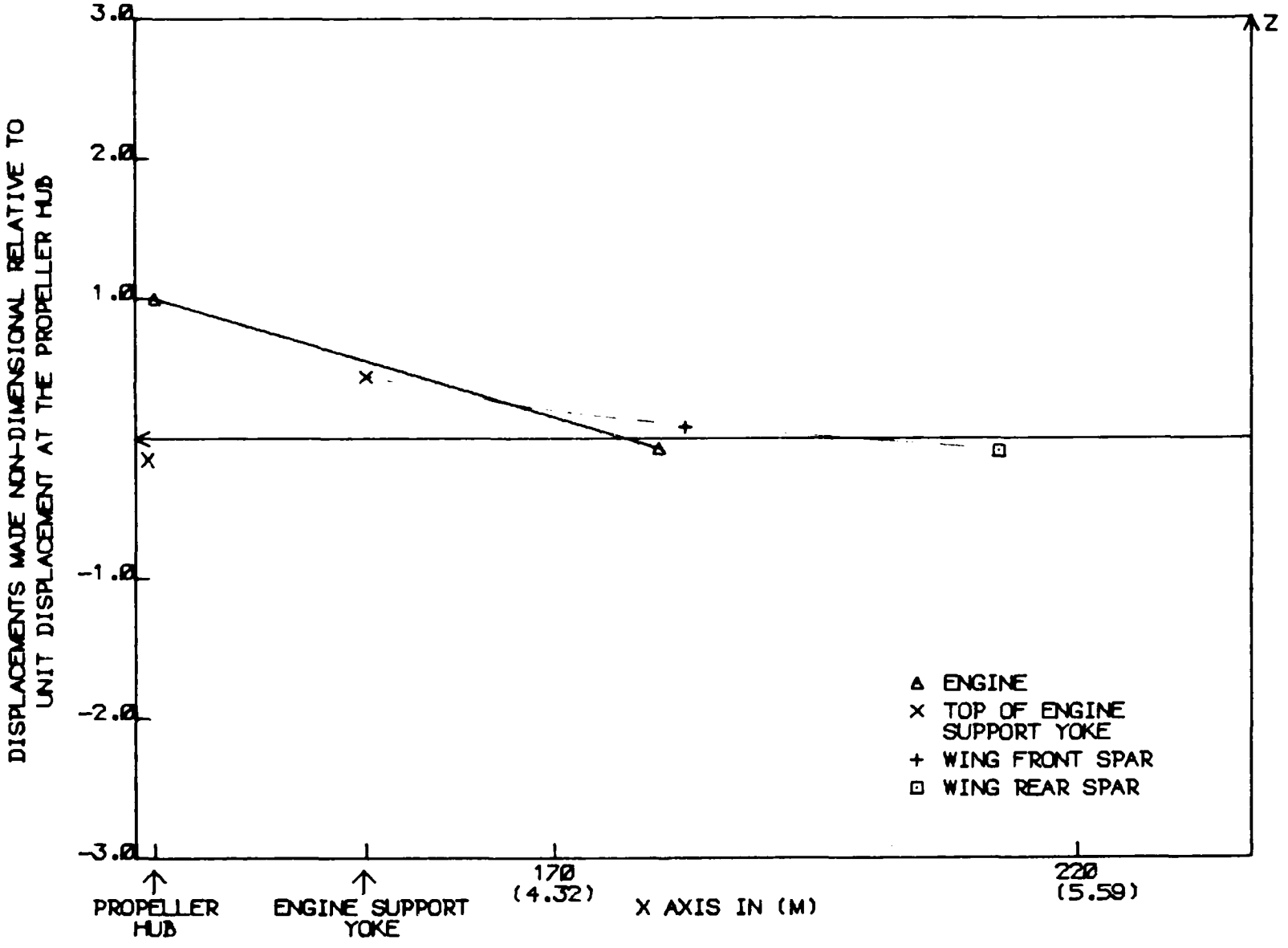

FIG. 4: ENGINE, NACELLE AND WING NON-DIMENSIONAL VERTICAL DISPLACEMENTS IN THE MODE AT 6·01 Hz.

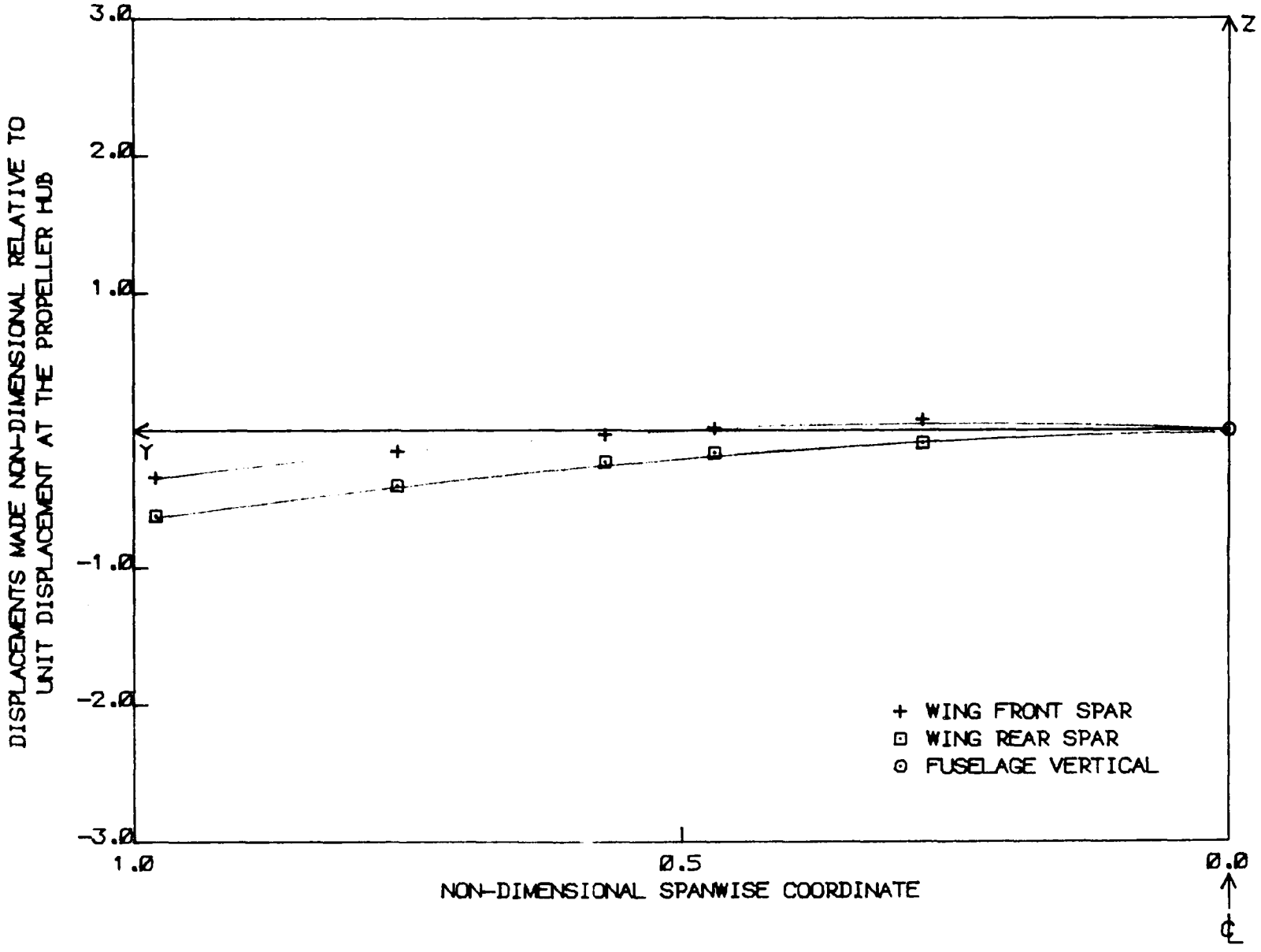

FIG. 5: WING BENDING IN THE MODE AT 6·01 Hz

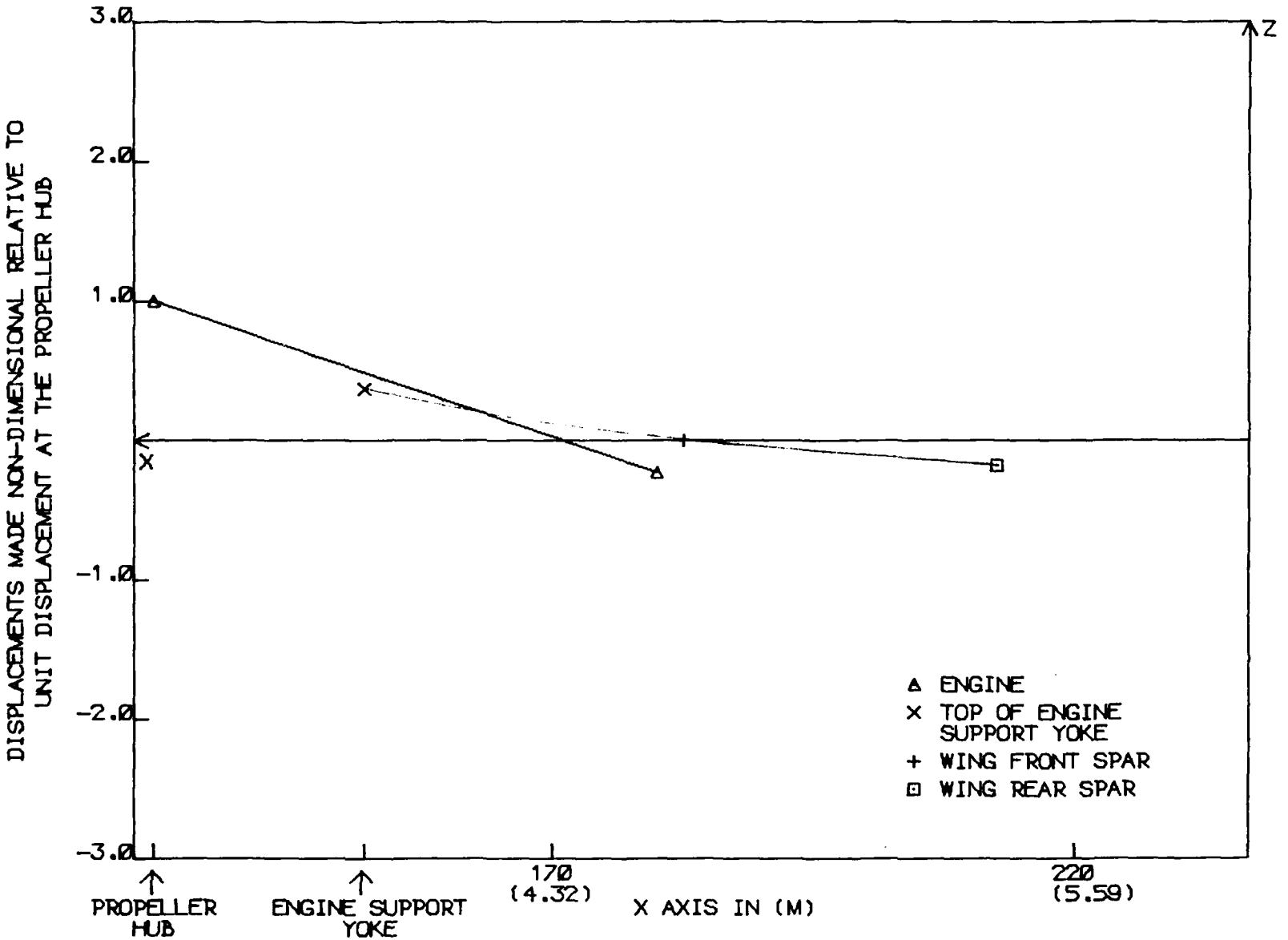

FIG. 6: ENGINE, NACELLE AND WING NON-DIMENSIONAL VERTICAL DISPLACEMENTS IN THE MODE AT 6·51 Hz

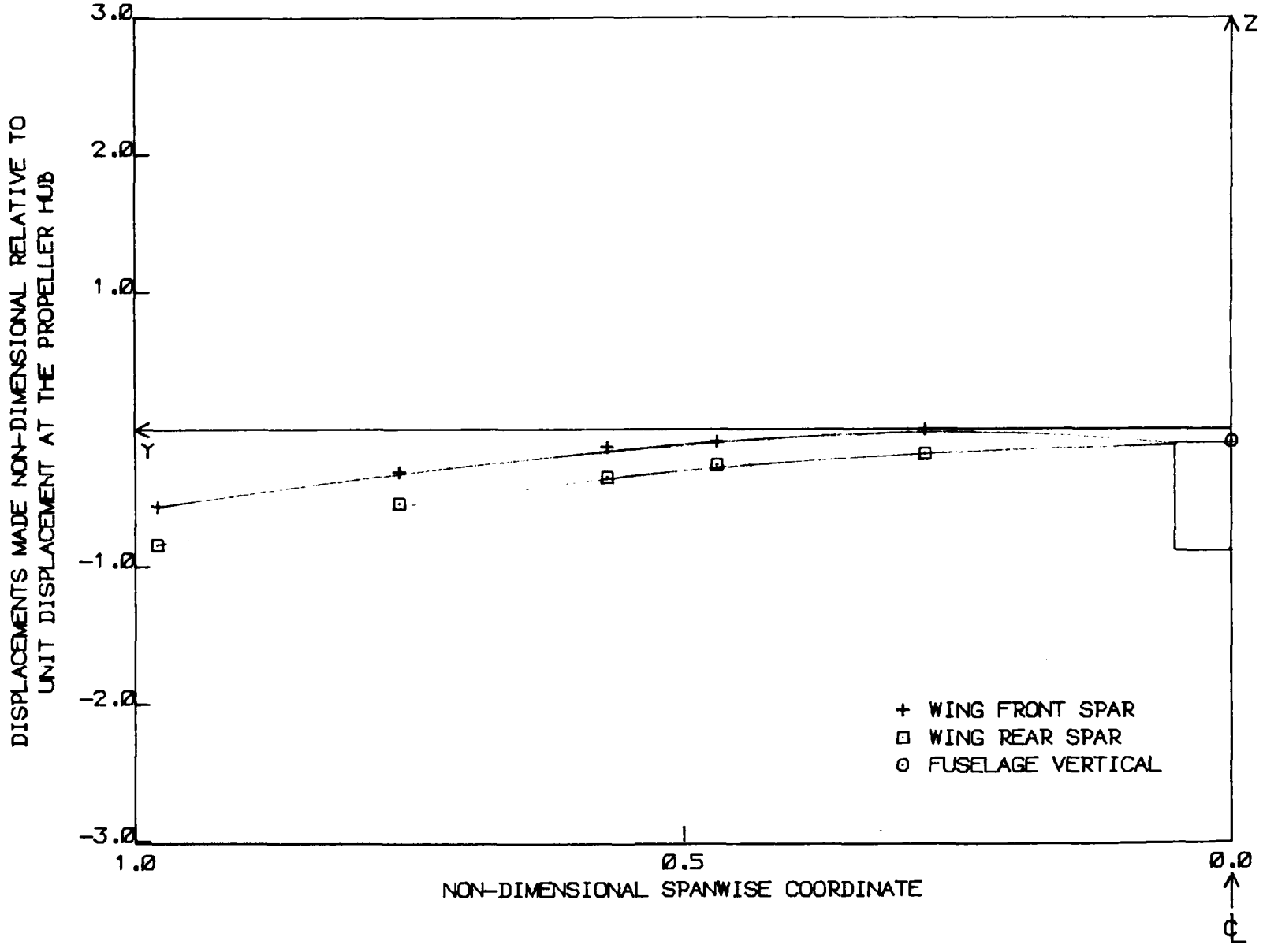

FIG. 7: WING BENDING IN THE MODE AT 6·51 Hz

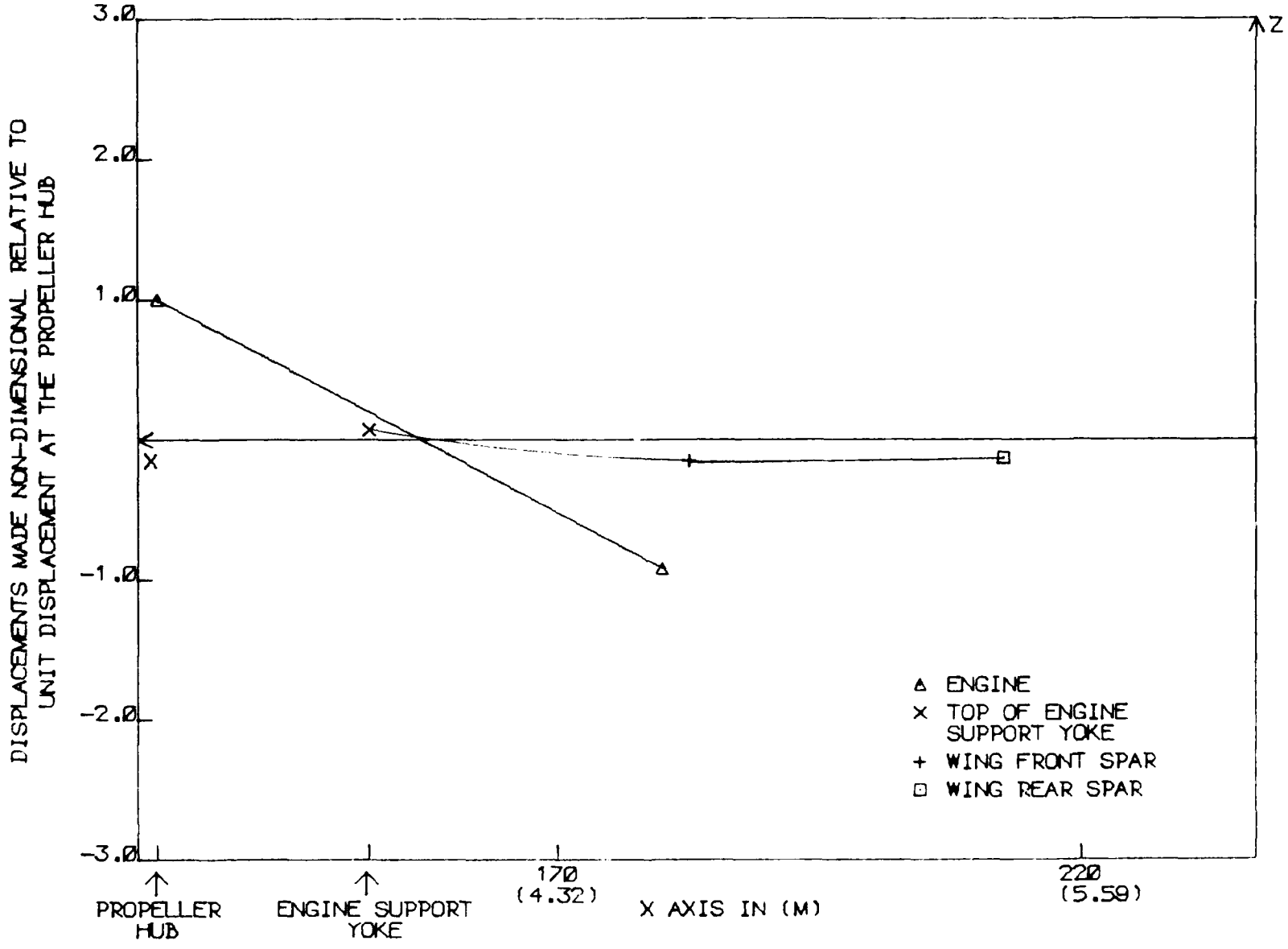

FIG 8 ENGINE NACELLE AND WING NON-DIMENSIONAL VERTICAL DISPLACEMENTS IN THE MODE AT 8·85 Hz

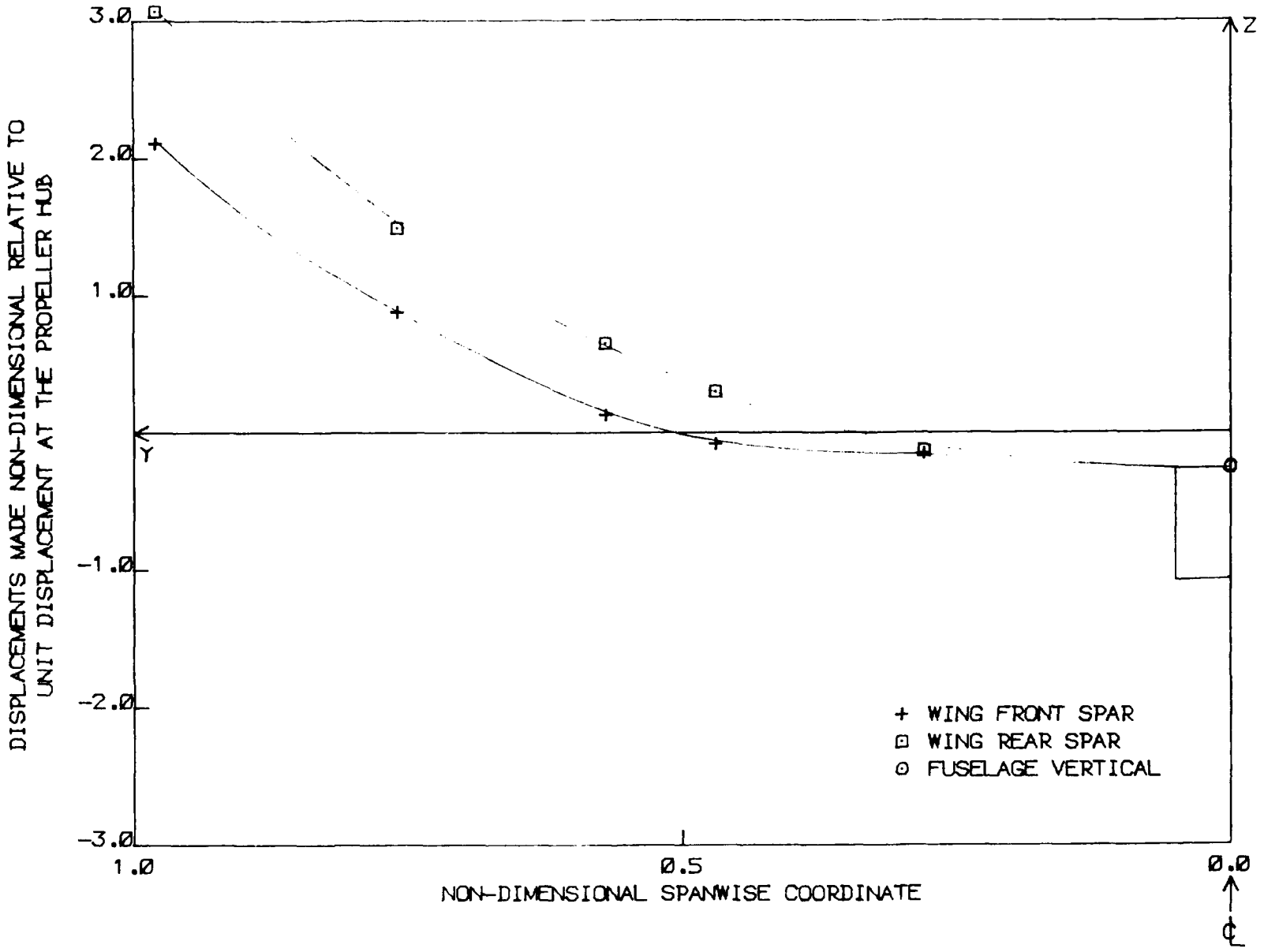

FIG. 9: WING BENDING IN THE MODE AT 8·85 Hz

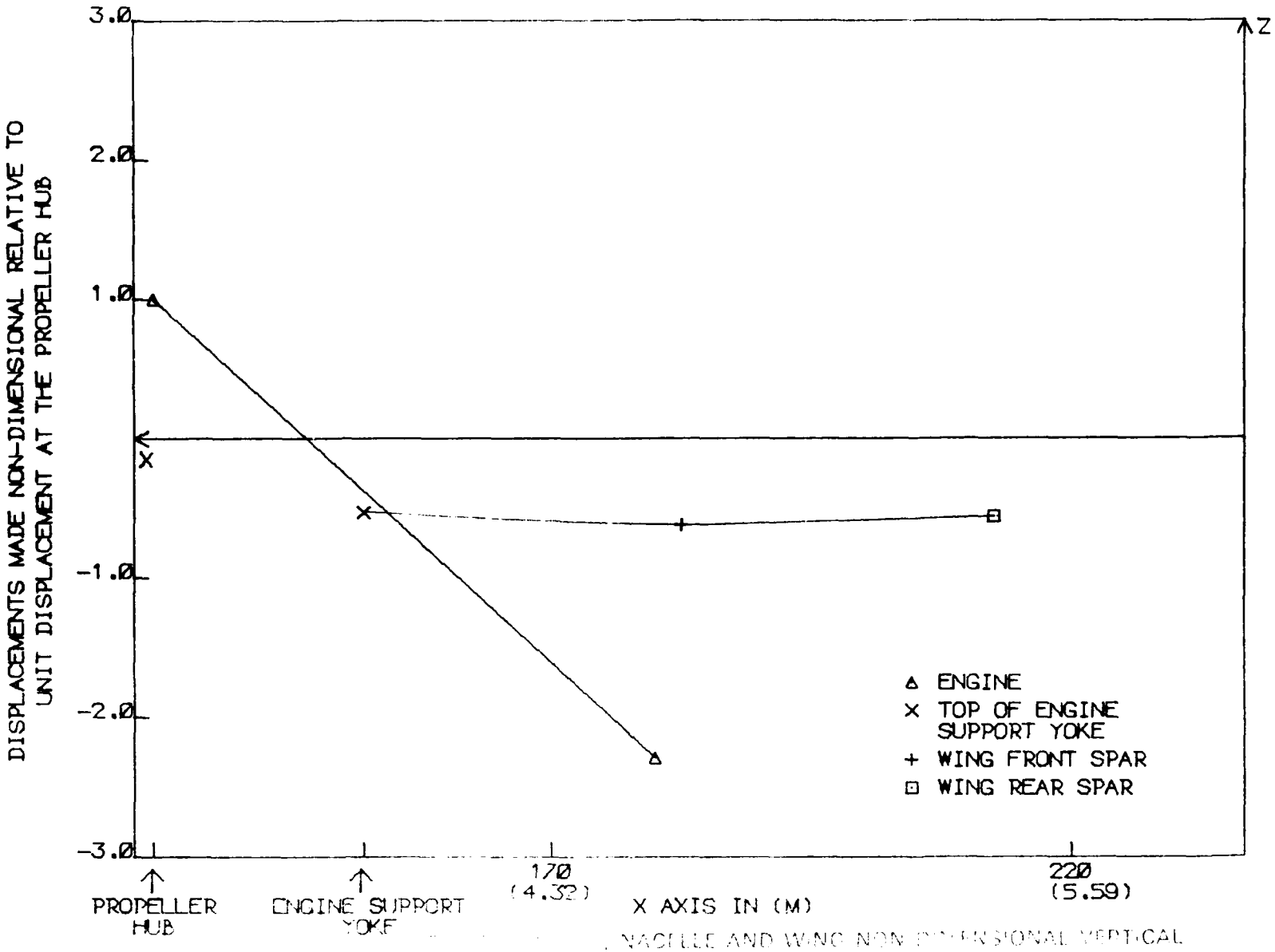

NACELLE AND WING NON-DIMENSIONAL VERTICAL

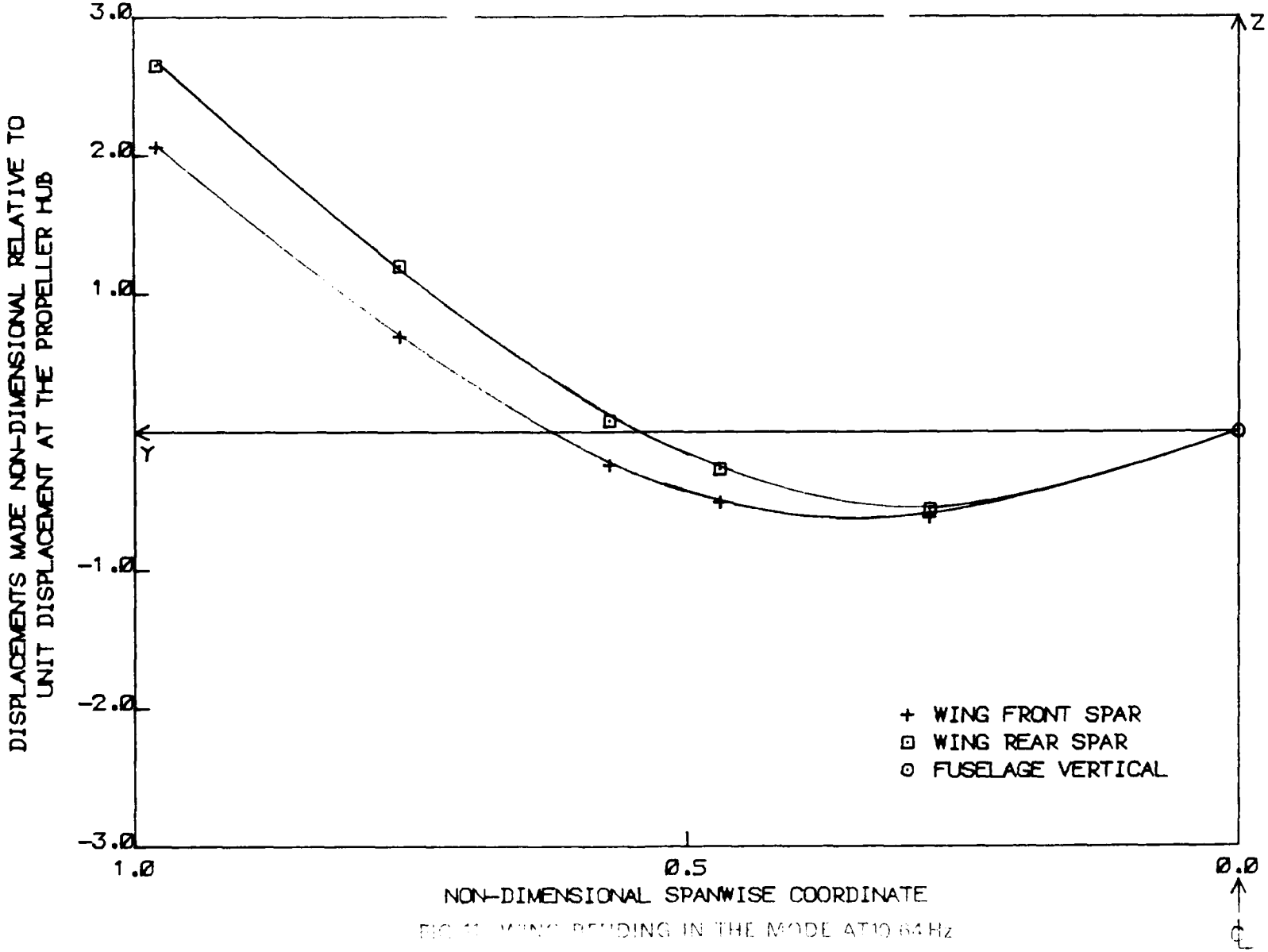

FIG 11 WING BENDING IN THE MODE AT 10.64 Hz

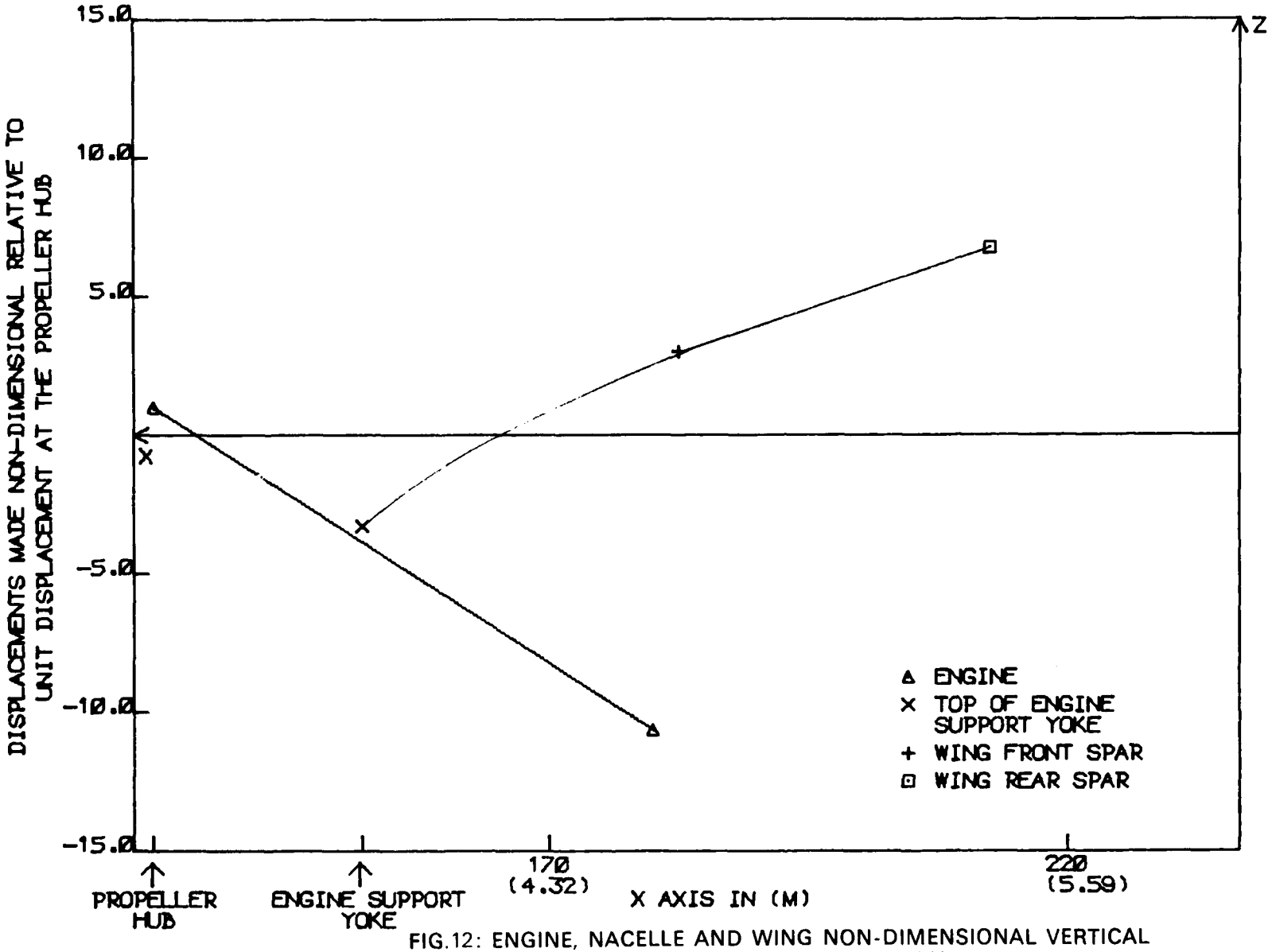

FIG.12: ENGINE, NACELLE AND WING NON-DIMENSIONAL VERTICAL DISPLACEMENTS IN THE MODE AT 15·40 Hz.

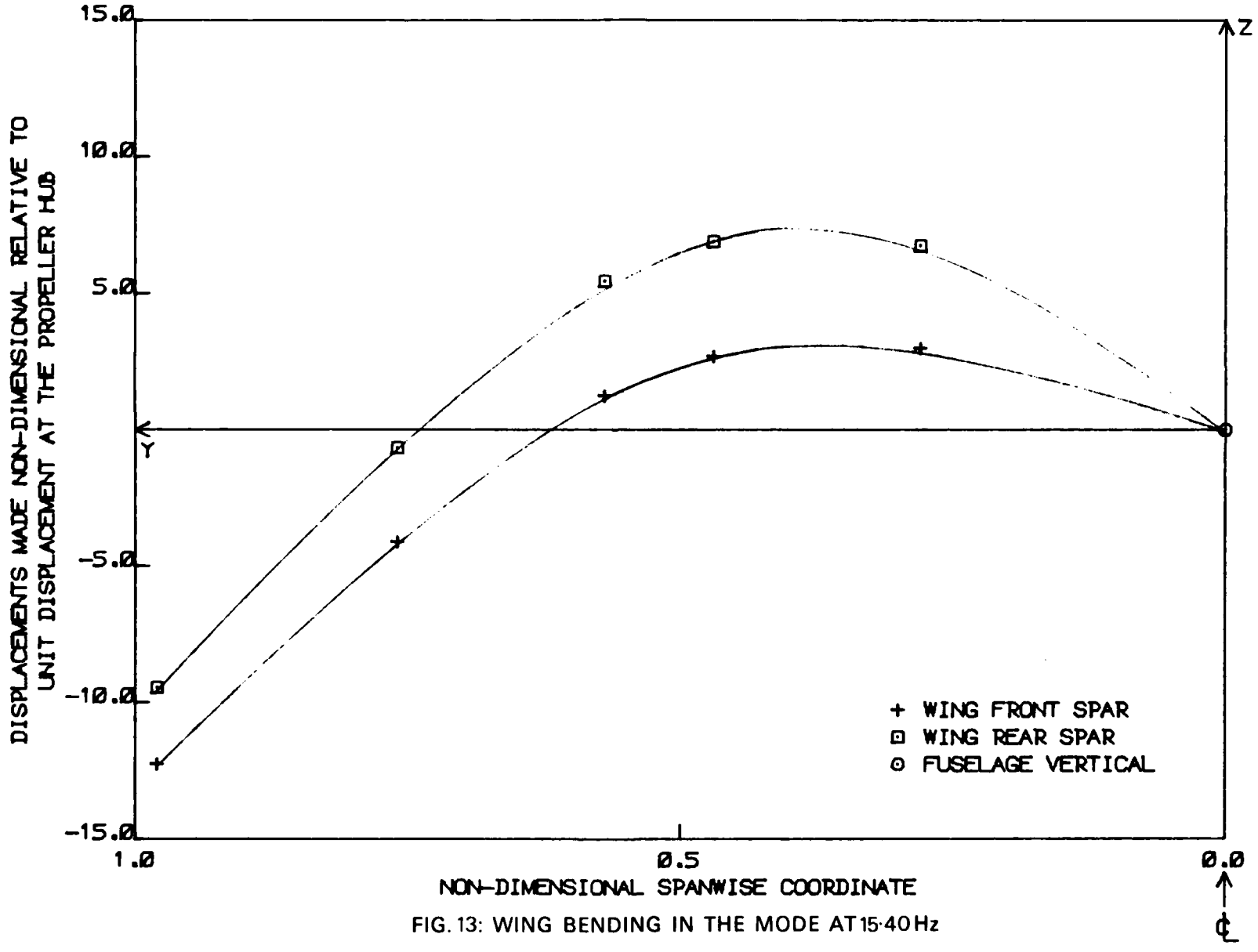

FIG. 13: WING BENDING IN THE MODE AT 15·40 Hz

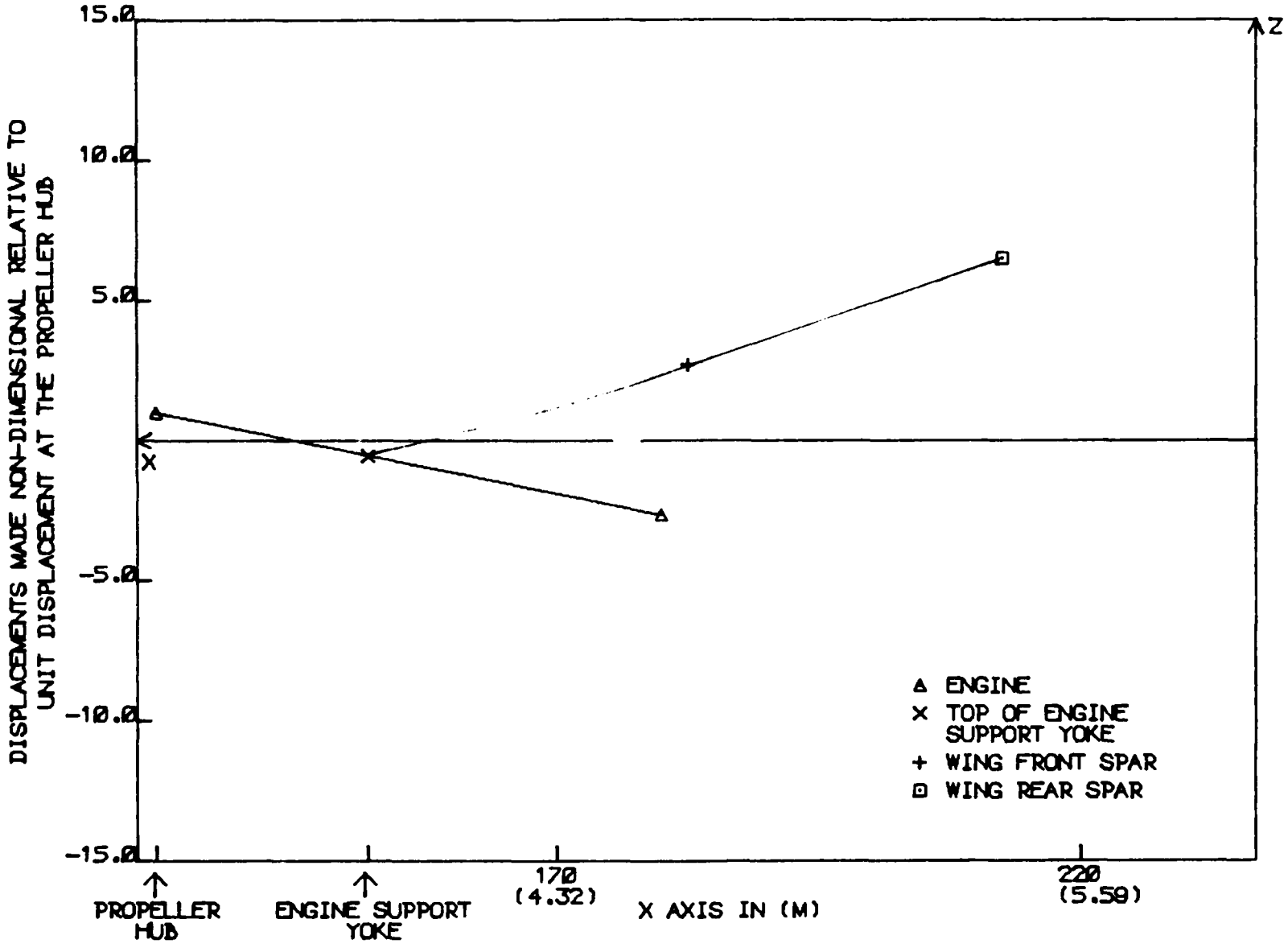

FIG. 14: ENGINE, NACELLE AND WING NON-DIMENSIONAL VERTICAL DISPLACEMENTS IN THE MODE AT 18·14 Hz

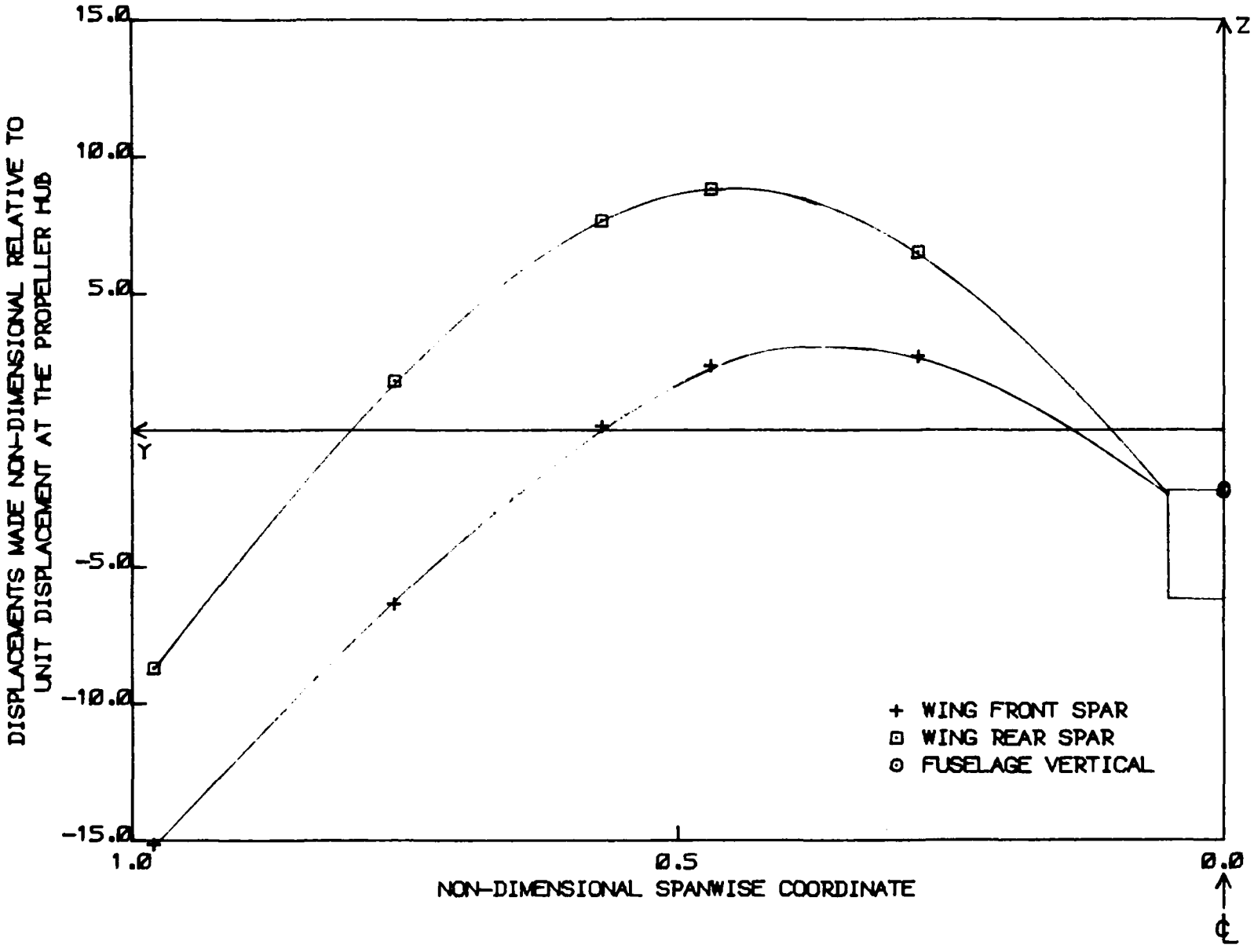

FIG. 15: WING BENDING IN THE MODE AT 18·14 Hz

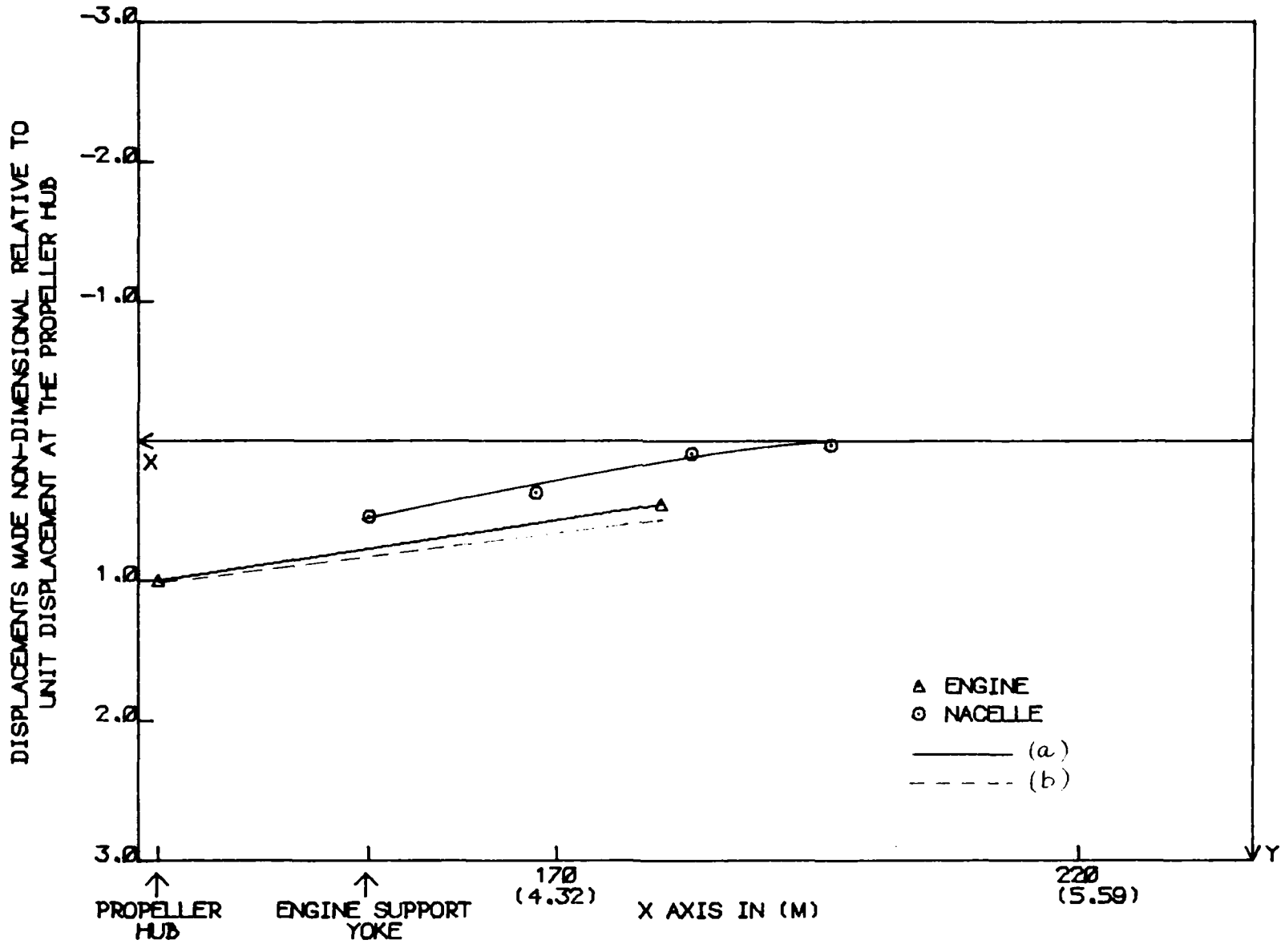

FIG. 16: ENGINE AND NACELLE NON-DIMENSIONAL HORIZONTAL DISPLACEMENTS IN THE YAW MODE AT 6·48 Hz

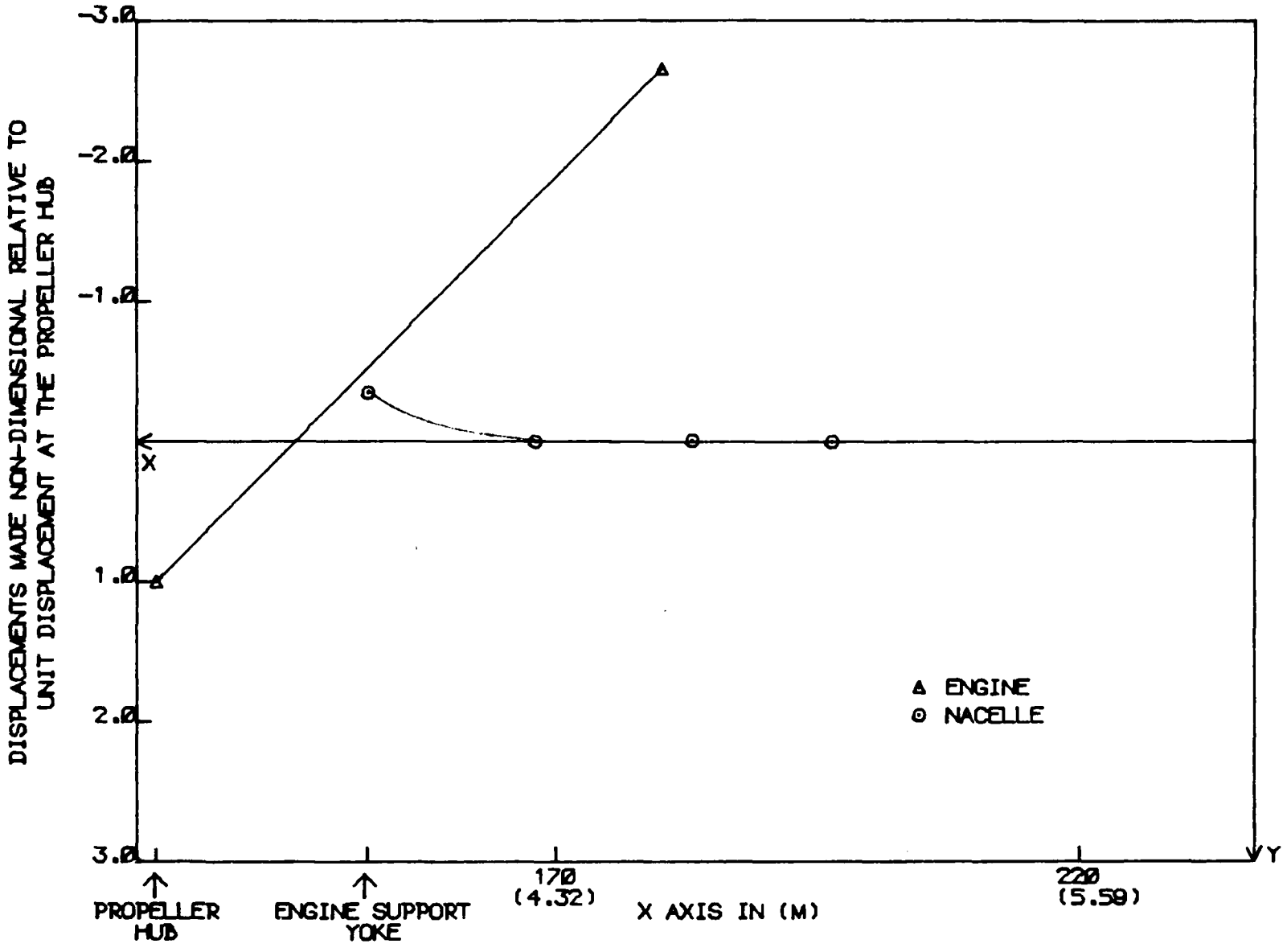

FIG. 17: ENGINE AND NACELLE NON-DIMENSIONAL HORIZONTAL DISPLACEMENTS IN THE YAW MODE AT 13·79 Hz

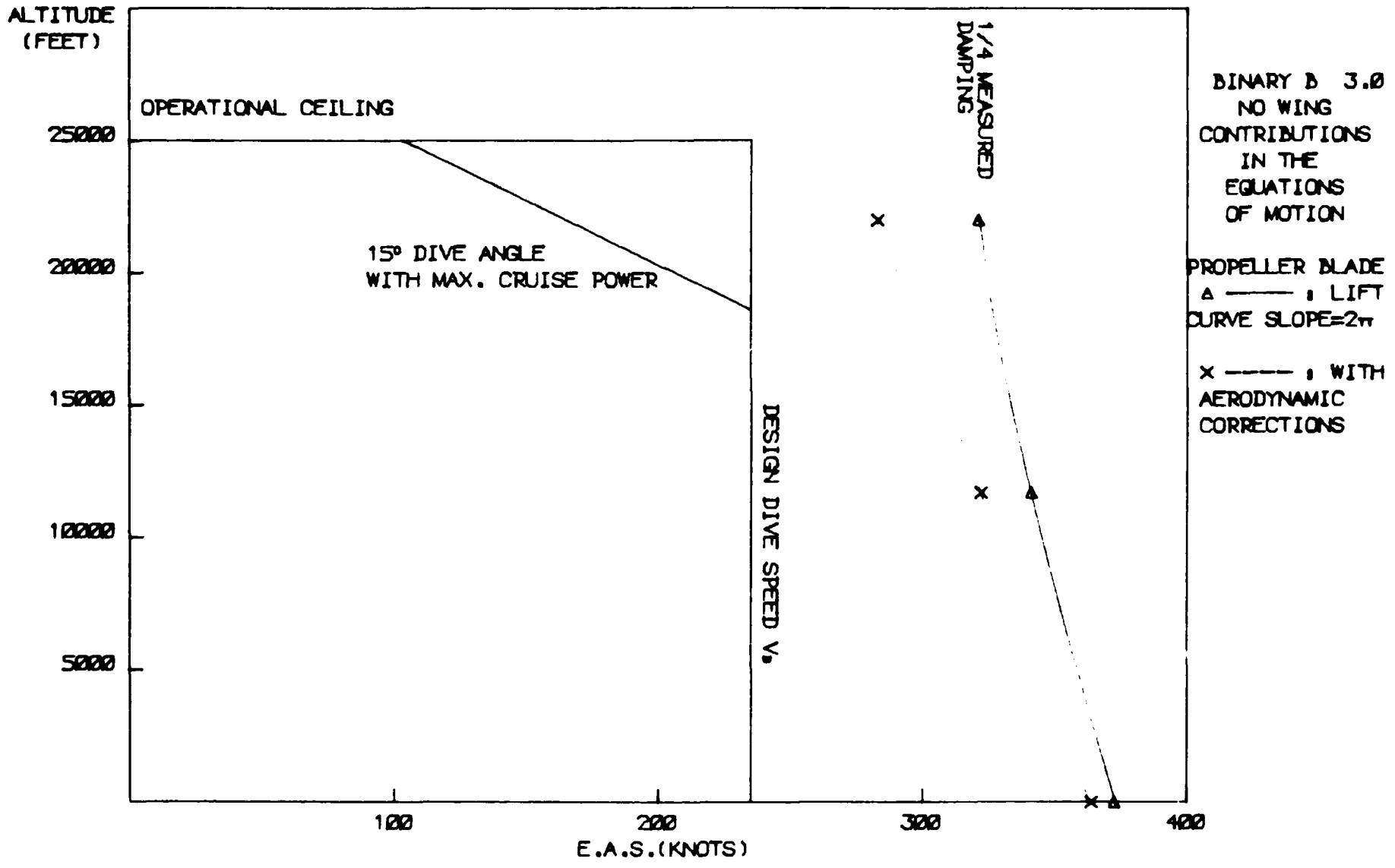

FIG. 18: WHIRL FLUTTER BOUNDARY

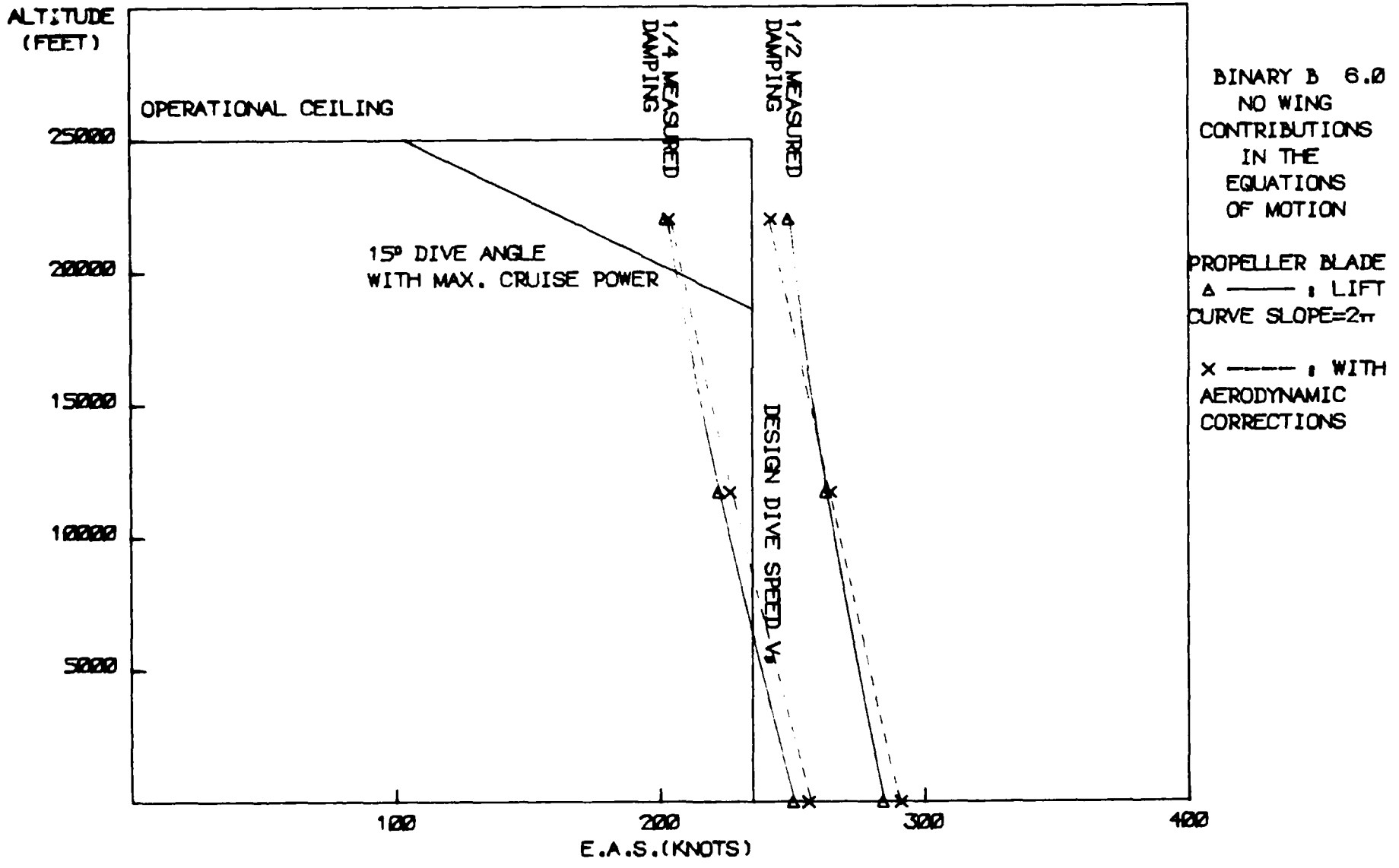

FIG. 19: WHIRL FLUTTER BOUNDARY

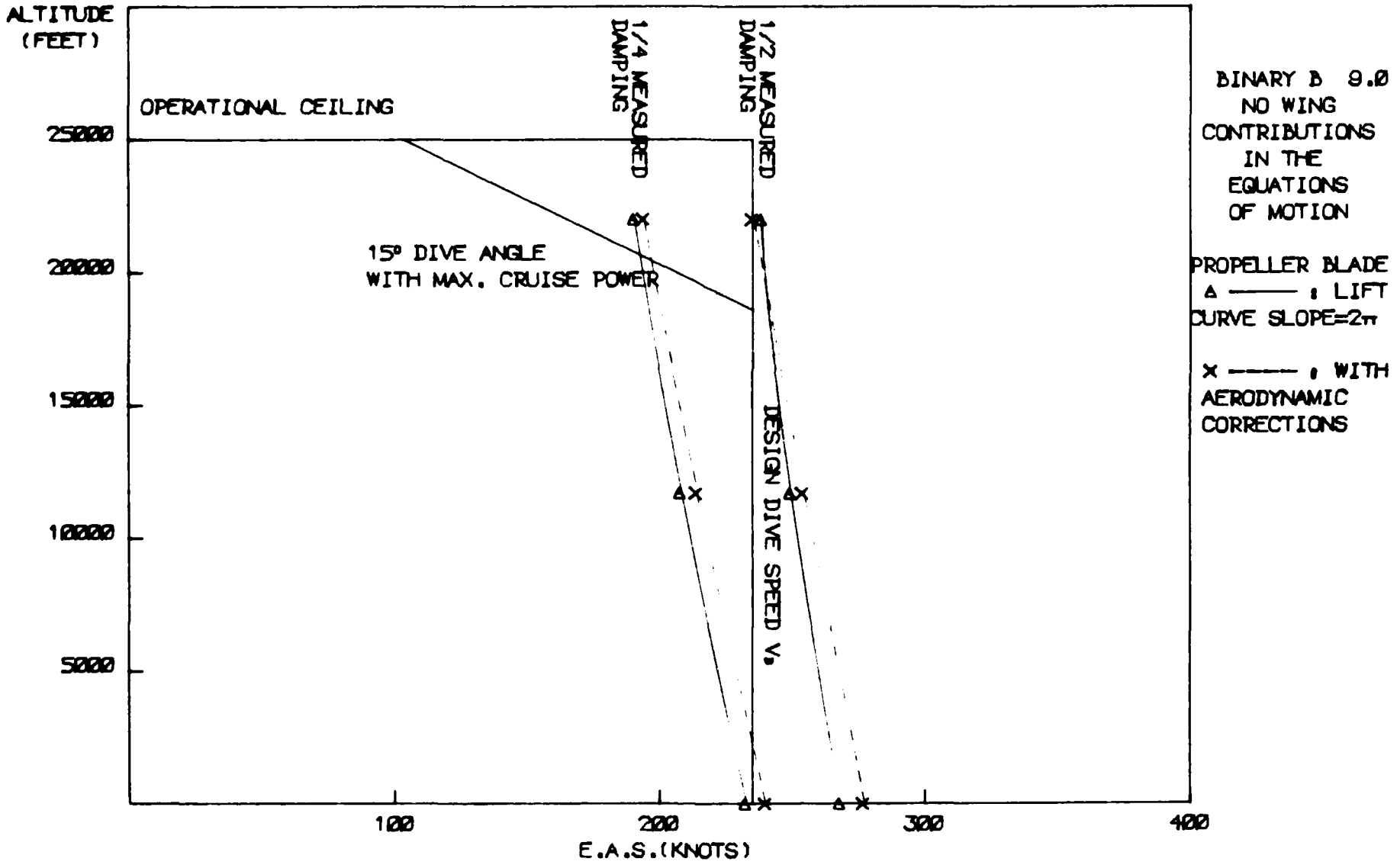

FIG. 20: WHIRL FLUTTER BOUNDARY

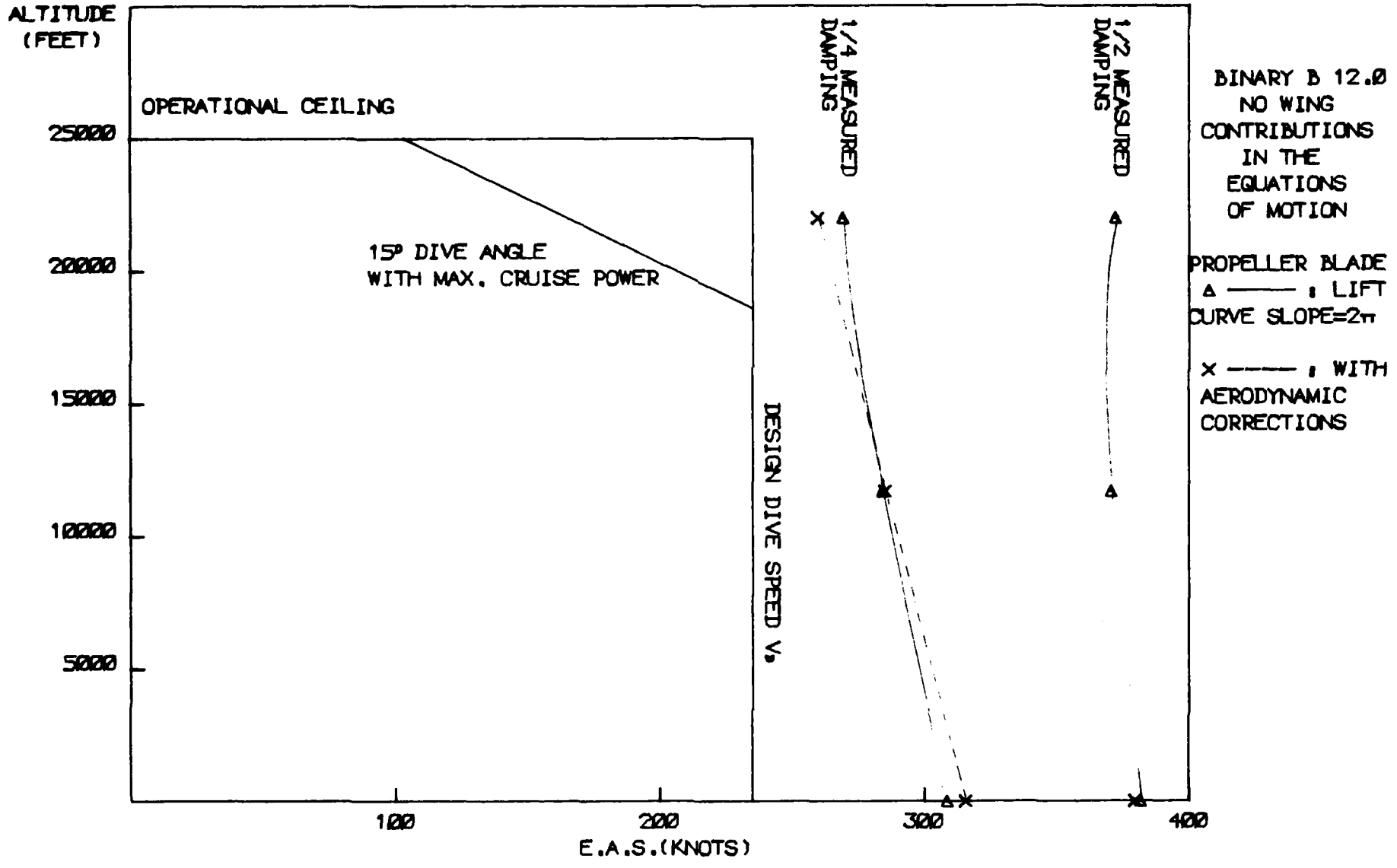

FIG. 21 : WHIRL FLUTTER BOUNDARY

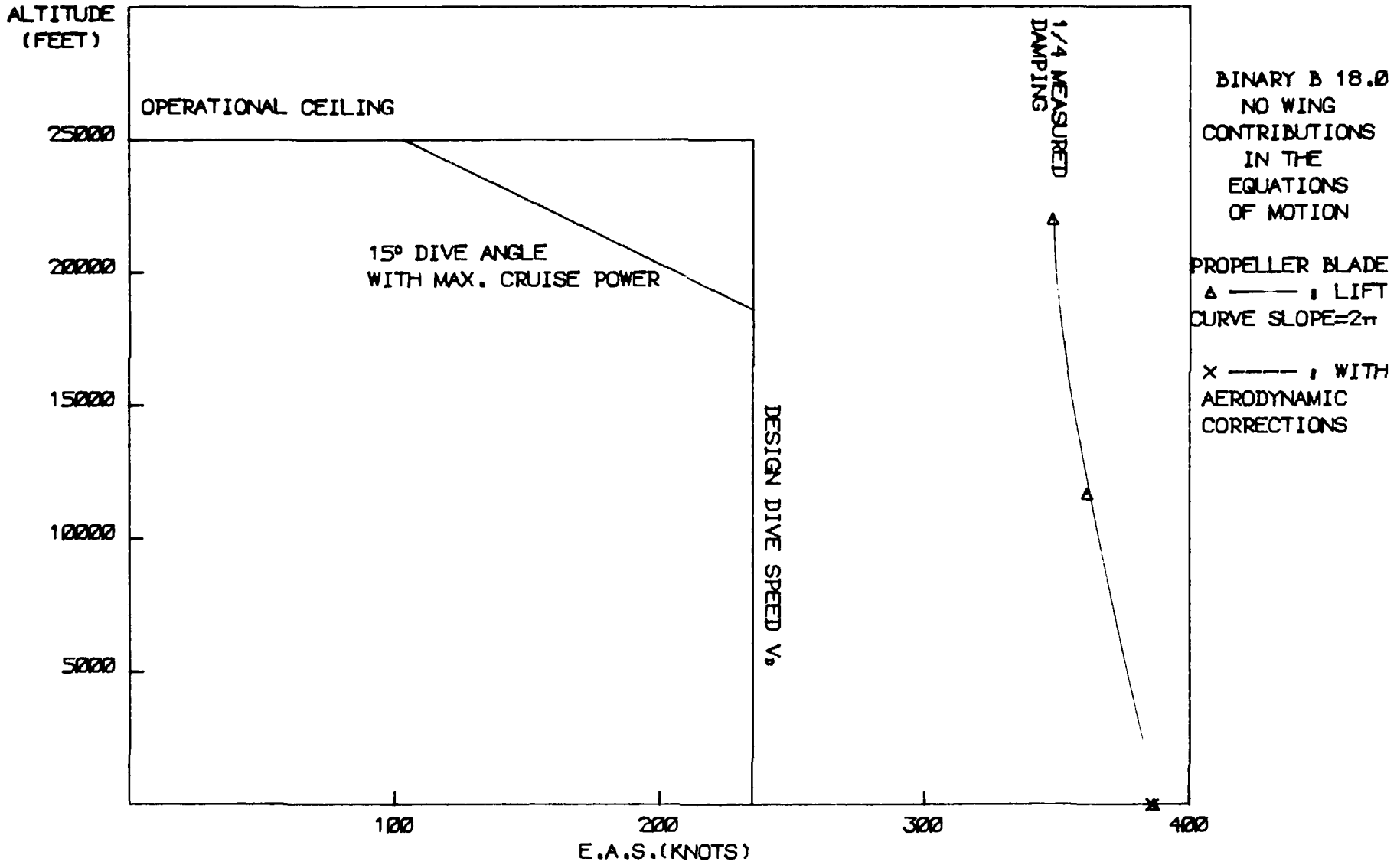

FIG. 22: WHIRL FLUTTER BOUNDARY

DISTRIBUTION

AUSTRALIA

Copy No.

Department of Defence

Central Office

Chief Defence Scientist	1
Deputy Chief Defence Scientist	2
Superintendent, Science and Technology Programs	3
Australian Defence Scientific and Technical Representative (U.K.)	4
Counsellor, Defence Science (U.S.A.)	5
Joint Intelligence Organisation	6
Defence Library	7
Assistant Secretary, D.I.S.B.	8 23

Aeronautical Research Laboratories

Chief Superintendent	24
Library	25
Superintendent, Structures Division	26
Structures Divisional File	27
Authors: Betty Emslie	28
Petra Cox	29
G. Long	30
N. B. Joyce	31
A. Goldman	32
P. A. Farrell	33
T. G. Ryall	34
B. Quinn	35

Materials Research Laboratories

Library	36

Defence Research Centre, Salisbury

Library	37

Central Studies Establishment

Information Centre	38

Engineering Development Establishment

Library	39

Army Office

Army Scientific Adviser	40

Air Force Office

Air Force Scientific Adviser	41
Aircraft Research and Development Unit, Scientific Flight Group	42
Technical Division Library	43
H.Q. Support Command (SENGSO)	44

Department of Productivity
Government Aircraft Factories

H. I. Gorjanicyn		45
P. F. Hughes		46
P. R. Scott		47
Library		48

Department of Transport

Secretary		49
Library		50
Airworthiness Group	R. Ferrari	51
	M. G. Chandivert	52

Spares 53–62

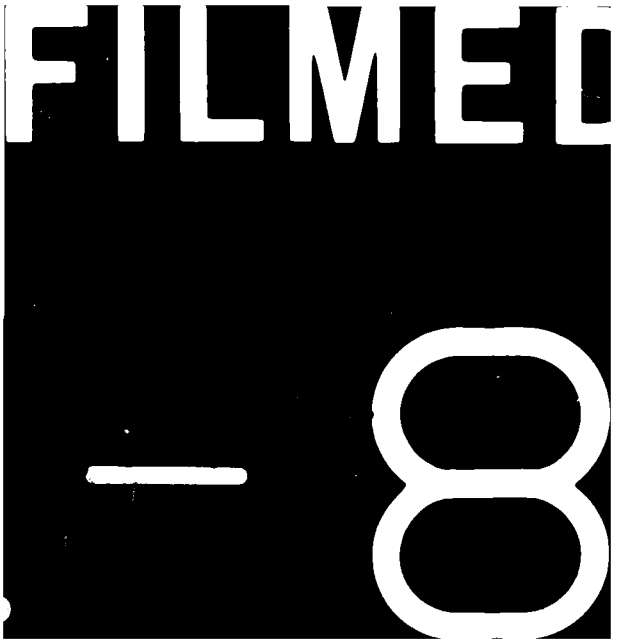
FILMED
8